








ORIGINAL RESEARCH

Thymidine Phosphorylase Deficiency or Inhibition Preserves Cardiac Function in Mice With Acute Myocardial Infarction

Lili Du , MD, PhD; Hong Yue , MD, PhD; Boyd R. Rorabaugh , PhD; Oliver Q. Y. Li, BA, BS, MS; Autumn R. DeHart ; Gretel Toloza-Alvarez , BA, BS, MS; Liang Hong, MD, PhD; James Denvir, PhD; Ellen Thompson , MD; Wei Li , MD, PhD

BACKGROUND: Ischemic cardiovascular disease is the leading cause of death worldwide. Current pharmacologic therapy has multiple limitations, and patients remain symptomatic despite maximal medical therapies. Deficiency or inhibition of thymidine phosphorylase (TYMP) in mice reduces thrombosis, suggesting that TYMP could be a novel therapeutic target for patients with acute myocardial infarction (AMI).

METHODS AND RESULTS: A mouse AMI model was established by ligation of the left anterior descending coronary artery in C57BL/6J wild-type and TYMP-deficient (*Tymp*^{-/-}) mice. Cardiac function was monitored by echocardiography or Langendorff assay. TYMP-deficient hearts had lower baseline contractility. However, cardiac function, systolic left ventricle anterior wall thickness, and diastolic wall strain were significantly greater 4 weeks after AMI compared with wild-type hearts. TYMP deficiency reduced microthrombus formation after AMI. TYMP deficiency did not affect angiogenesis in either normal or infarcted myocardium but increased arteriogenesis post-AMI. TYMP deficiency enhanced the mobilization of bone marrow stem cells and promoted mesenchymal stem cell (MSC) proliferation, migration, and resistance to inflammation and hypoxia. TYMP deficiency increased the number of larger MSCs and decreased matrix metalloproteinase-2 expression, resulting in a high homing capability. TYMP deficiency induced constitutive AKT phosphorylation in MSCs but reduced expression of genes associated with retinoid-interferon-induced mortality-19, a molecule that enhances cell death. Inhibition of TYMP with its selective inhibitor, tipiracil, phenocopied TYMP deficiency, improved post-AMI cardiac function and systolic left ventricle anterior wall thickness, attenuated diastolic stiffness, and reduced infarct size.

CONCLUSIONS: This study demonstrated that TYMP plays an adverse role after AMI. Targeting TYMP may be a novel therapy for patients with AMI.

Key Words: acute myocardial infarction ■ mesenchymal stem cells ■ stem cell therapy ■ thrombosis ■ thymidine phosphorylase

Ischemic cardiovascular disease is the leading cause of death worldwide. This may result from the increased prevalence of metabolic disorders including obesity, nonalcohol fatty liver diseases, and type 2 diabetes, all are risk factors for ischemic cardiovascular disease.¹ In these disease conditions, atherosclerotic plaques accumulate. When plaque ruptures, a thrombus forms and occludes the coronary artery. This leads to acute

myocardial infarction (AMI) and myocardial cell death. While revascularization strategies (including coronary artery bypass grafting, percutaneous transluminal coronary angioplasty, and medicine-mediated thrombolytic therapies) have achieved significant progression and dramatically reduced ischemic cardiovascular disease-associated mortality, about 30% of patients with the ischemic cardiovascular disease still develop chronic

Correspondence to: Wei Li, MD, PhD, Department of Biomedical Sciences, BBSC 241G, Joan C. Edwards School of Medicine, Marshall University, One John Marshall Dr, Huntington, WV 25755-9310. Email: liwe@marshall.edu

Supplemental Material is available at <https://www.ahajournals.org/doi/suppl/10.1161/JAHA.122.028023>

For Sources of Funding and Disclosures, see page 17.

© 2023 The Authors. Published on behalf of the American Heart Association, Inc., by Wiley. This is an open access article under the terms of the [Creative Commons Attribution-NonCommercial-NoDerivs](https://creativecommons.org/licenses/by-nc-nd/4.0/) License, which permits use and distribution in any medium, provided the original work is properly cited, the use is non-commercial and no modifications or adaptations are made.

JAHA is available at: www.ahajournals.org/journal/jaha

CLINICAL PERSPECTIVE

What Is New?

- Our study demonstrated that deficiency or inhibition of thymidine phosphorylase improved cardiac function in mice under acute myocardial infarction.
- Our study also demonstrated that deficiency or inhibition of thymidine phosphorylase enhanced the function of mesenchymal stem cells.

What Are the Clinical Implications?

- Inhibition of thymidine phosphorylase with a US Food and Drug Administration-approved inhibitor, namely tipiracil hydrochloride, may reduce myocardial infarction size and enhance cardiac function.
- The antiplatelet and antithrombotic function of tipiracil is rapid and safe, which could be a novel regimen for patients with onset acute myocardial infarction or for patients who need immediate antiplatelet intervention.

Nonstandard Abbreviations and Acronyms

AAR	areas at risk
BM	bone marrow
CM	complete media
DWS	diastolic wall strain
LG-DMEM	low-glucose DMEM
LVAW	left ventricle anterior wall
LVPWs	systolic left ventricle posterior wall
LVPWd	diastolic left ventricle posterior wall
MMP	matrix metalloproteinase
MSCs	mesenchymal stem cells
TYMP	thymidine phosphorylase
VSMC	vascular smooth muscle cells

heart failure following myocardial infarction.² It has been estimated that >6.2 million Americans ≥ 20 years of age have had heart failure, and the prevalence is consistently increasing.³ The necrotic area of the heart is a determining factor in the long-term prognosis. Therefore, the salvaging of ischemic myocardium and suppression of myocardial remodeling are highly desirable.⁴ Current pharmacological therapy for ischemic heart disease has multiple limitations including patient compliance issues and drug side effects. Revascularization procedures often end with the need for repeat procedures. Patients remain symptomatic despite maximal medical therapy.⁵ To this end, gene and/or stem cell therapies, including using mesenchymal stem cells (MSCs), have been

developed and provide promising preclinical results. However, clinical data still do not fully indicate that these methods have significant clinical benefits.

Therapeutic angiogenesis seeks to improve tissue perfusion in chronic diseases through the growth and proliferation of blood vessels in response to the delivery of angiogenic cytokines, such as vascular endothelial growth factor or hepatocyte growth factor. However, a phase II, randomized, double blind-controlled study of adenoviral delivery of vascular endothelial growth factor 121 in patients with peripheral artery disease did not find improved exercise performances or quality of life.⁶ In addition to the proangiogenic genes, gene transfer of an antiapoptotic factor Bcl-2,⁷ or a cytoprotective gene, heme oxygenase-1, also reportedly protects hearts from late postischemic heart failure.⁸ Furthermore, inflammatory responses post-AMI play important roles in determining infarct size and subsequent adverse cardiac remodeling.⁹ While results from CANTOS (Canakinumab Anti-inflammatory Thrombosis Outcomes Study) showed modest benefits,¹⁰ CIRT (Cardiovascular Inflammation Reduction Trial)¹¹ and COLCOT (Colchicine Cardiovascular Outcomes Trial)¹² showed no benefits for the cardiovascular outcome, raising the question of whether direct intervention on inflammation can improve cardiovascular outcomes.

The identification of stem cells in the cardiovascular system makes them a potential option to develop novel cell-based therapies. Among them, MSCs have drawn the attention of scientists because of their broad spectrum of capabilities for tissue repair.^{13,14} Accumulating evidence indicates that the therapeutic effects of MSCs are mainly through their paracrine effects,¹⁵ including inflammation reduction and immunomodulation.^{16,17} Although MSCs are mainly isolated from bone marrow (BM), adipose-derived MSCs have been recognized as an alternative source of BM-derived MSCs for usage in therapeutic applications.¹⁸ However, some main problems including delivery methods, low degree of retention of MSCs in the tissues, and short-lived viability after implantation remain to be solved.¹⁹

Thymidine phosphorylase (TYMP), also known as platelet-derived endothelial cell growth factor, is an enzyme that reversibly catalyzes the action of thymidine to thymine and 2-deoxy-D-ribose-1-phosphate and plays a role in maintaining the balance of the nucleotide pool of these molecules.²⁰ TYMP has proangiogenic activity *in vivo*. It stimulates the chemotaxis of endothelial cells and confers resistance to apoptosis induced by hypoxia. We have examined the therapeutic effects of the transfection of TYMP gene to the chronic ischemic myocardium, and the effects were studied for as long as 6 months in dogs.^{4,21} We also found that gene transfection of TYMP into rat or rabbit vascular smooth muscle cells (VSMCs) dramatically inhibited VSMCs proliferation by increasing the expression of heme oxygenase-1 and p27 and

through regulating the activity of Lyn kinase.^{22–24} The antioxidative heme oxygenase-1 has been confirmed to reduce ischemic injury in most animal models including the heart, brain, and liver.²⁵ All of these data suggest that TYMP could be a useful gene for the treatment of myocardial ischemia by promoting angiogenesis, inhibiting apoptosis, and preventing the proliferation of VSMCs. However, our recent study also demonstrated that TYMP deficiency in mice or TYMP inhibition with its potent and selective inhibitor tipiracil, significantly inhibited thrombosis in mice.^{26,27} These data suggest that TYMP deficiency or inhibition may also benefit AMI by reducing microthrombosis and infarction-related inflammation, thus attenuating ischemia-associated complications. The comprehensive effects of TYMP after AMI, however, have never been systemically studied.

METHODS

The authors declare that all supporting data are available within the article. The data that are marked as “Data not shown” are available from the corresponding author upon reasonable request.

Experiment Animals

Wild-type (WT) C57BL/6J breeding mice were purchased from the Jackson Laboratory (Bar Harbor, ME). The *Tymp*^{-/-} mouse strain was produced by Dr. Hirano, and it has been backcrossed onto the C57BL/6J background >10 times and used in our studies before.^{26–28} Mice had ad libitum access to Laboratory Rodent Diet (LabDiet, Cat# 5001,) and water and were housed in a fully AAALAC-accredited animal facility with 12:12 dark and light cycle. Since sex hormones have a significant effect on the development of cardiovascular diseases, only male mice were used for the comparison of the role of TYMP on AMI in vivo. Some experiments that are not affected by sex hormones used both sexes, which has been indicated in the results. All procedures and manipulations of animals have been approved by the IACUC at Marshall University (IACUC#: 1033528).

Murine AMI Model

Mice 10 to 12 weeks of age were anesthetized with ketamine/xylazine (100/10 mg/kg). Mice were intubated and ventilated with 100% oxygen at a breath rate of 110/min and a tidal volume of 120–150 μ L (MiniVent Ventilator for Mice, Harvard Apparatus). Eye lubricant was applied, and mice were fixed in the supine position on a warm operating plate. Body temperature (37 $^{\circ}$ C) was monitored with an anal probe monitor. The hair on the left chest was shaved followed by treating with hair removal cream. The operation site was disinfected using Povidone-Iodine Prep Pad followed by wiping with 70% ethanol. The heart was exposed through

a left thoracotomy between the third and fourth ribs. The pericardial sac was cut open and the left anterior descending coronary artery (LAD) was ligated at the level \approx 3mm below the left atrial appendix with an 8–0 Prolene polypropylene suture. The success of the LAD ligation was confirmed by identifying the myocardium distal to the ligation site turning pale. A small drain tube with multiple holes on the tip was placed into the chest cavity, and the chest was closed using a 5–0 Coated Vicryl Plus suture (Ethicon, Somerville, NJ). Immediately before applying the last suture for closing the chest, the lungs were inflated and air remaining in the chest cavity was removed. The drain tube was removed, and the mice were kept warm until they returned to spontaneous breathing. The intubation tube was removed, and mice were kept in a clean warm cage overnight. Buprenorphine (0.05 mg/kg) was administered immediately after the surgery and then twice per day for 3 days. Mice were monitored twice daily for the first 3 days, and then once per day for the first week, and then housed as normal.

Mice were euthanized at 1, 3, 7, or 28 days by either an overdose of ketamine/xylazine (200/20 mg/kg) or a bolus of KCl (150 mg/kg) depending on the individual type of experiments as indicated in the Results section. Hearts were rinsed in cold PBS and processed for future biochemical and histological examinations. Some WT mice were orally fed tipiracil for 1 week to inhibit TYMP activity before they were subjected to ligation of the left anterior descending coronary artery. Tipiracil (1 mg/kg) was continually administered once daily for 28 days before harvesting the hearts.

Echocardiography

Echocardiography was conducted using the Vevo 1100 Imaging System (FUJIFILM VisualSonics) with an MS400 18–38 MHz transducer before the surgery and 7 and 28 days after AMI. Mice were anesthetized with ketamine/xylazine (100/10 mg/kg), and hair on the chest was removed with hair removal cream. The animal was fixed on a temperature-controlled ECG plate in the supine position, and its heart rate was monitored. Echo data were collected at the heart rate range around 280 to 350/min, and 2-dimensional guided M-mode was used for evaluating cardiac function.^{29,30} All data were analyzed with the software associated with the Vevo 1100. Diastolic wall strain (DWS) was calculated using the systolic and diastolic left ventricle posterior wall (LVPWs and LVPWd) thickness using the following equation: $DWS = (LVPWs - LVPWd)/LVPWs$.^{31,32}

Langendorff Isolated Heart Experiments

Mice received a single intraperitoneal injection containing pentobarbital (150 mg/kg) and heparin (60 mg/kg). Hearts were rapidly removed from the

anesthetized animals, mounted on a Langendorff isolated heart system, and perfused with Krebs solution (in mmol/L: 118 NaCl, 4.7 KCl, 1.2 MgSO₄, 25 NaHCO₃, 1.2 KH₂PO₄, 0.5 Na₂EDTA, 11 glucose, 2.5 CaCl₂, pH 7.4) at a constant pressure of 70 mmHg as previously described.³³ Contractile function of the left ventricle was measured by an intraventricular balloon connected to a pressure transducer, and data were continuously recorded by a PowerLab 4SP data acquisition system (AD Instruments, Colorado Springs, CO). The temperature of the heart (37 °C) was monitored by a temperature probe placed on the surface of the heart. Following 15 minutes of perfusion, the LAD was ligated with an 8–0 suture. Parameters of cardiac function, including heart rate, developed pressure, \pm dP/dt, and coronary flow rate, were recorded immediately before and 10 minutes after LAD ligation. Hearts were excluded after the 15-minute equilibration period if the flow rate was >5.0 mL/min (indicative of an aortic tear), developed pressure <50 mmHg, heart rate <200 beats/min, or if there were persistent arrhythmias.

Evans Blue and Triphenyl Tetrazolium Chloride Staining

The mouse was anesthetized with ketamine/xylazine (100/10 mg/kg), and the heart was stopped in the diastolic phase by bolus intravenous injection of KCl solution (150 mg/kg). The heart was removed, rinsed with cold PBS, and frozen at –20 °C for 30 minutes. The frozen heart was then sliced into pieces in 1-mm sections and sequentially placed into wells of a 24-well plate. The heart slices were incubated in 2 mL 2% triphenyl tetrazolium chloride solution for 15 minutes in a 37 °C water bath, washed with PBS, flattened on a slide glass, and images were taken.

Some mice were euthanized 18 hours after LAD ligation to identify areas at risk (AAR) and infarct areas in the early phase. To this end, the mouse heart was rapidly removed and mounted to a perfusion system by cannulating and ligating the aorta to a 25-G blunt needle. The hearts were perfused with cold PBS, followed by 3 mL, 0.22 μ m filtered, 0.8% Evans blue in saline. The hearts were rinsed with cold PBS and then stained with triphenyl tetrazolium chloride as mentioned above. The ischemic area and infarct size were measured using ImageJ. Data were presented using definitions shown in the corresponding figure legends.

Quantitative Polymerase Chain Reaction

Total RNA was isolated from infarcted myocardium using the Qiagen Universal RNA extraction kit. RNA concentration was measured using a NanoDrop, and 1 μ g of total RNA was used for cDNA construction using the Super Script VILO cDNA Synthesis Kit

(ThermoFisher Scientific, Waltham, MA). Table S1 lists the primers used for analyzing the expression of inflammatory cytokines. PowerUp SYBR Green Master Mix (ThermoFisher) was used for quantitative polymerase chain reaction analysis using the ABI SimpliAmp Thermal Cycler.

Histological Analysis

Serial 4- to 5- μ m thick paraffin-embedded sections were cut for histological examination. Immunohistochemical or immunofluorescence staining was performed using antibodies against CD31 (SC-376764, Santa Cruz), α -smooth muscle actin (A2547, Sigma-Aldrich), and cleaved caspase-3 (9664 S, Cell Signaling). Frozen heart sections prepared 24 hours after AMI were stained for CD41 (Cat #553847, BD Pharmingen) to identify microthrombosis and α -smooth muscle actin to quantitatively analyze arteriogenesis at the early phase of AMI.

Murine Adipose-Derived Mesenchymal Stem Cell Isolation and Culture

Murine MSCs were cultured as previously described.^{34,35} Male mice were euthanized and perigonadal fat pads were harvested, rinsed with ice-cold PBS, and soaked in 5 \times antibiotic-containing PBS for 10 minutes on ice. Fat tissues were minced and digested with 0.1% collagenase I in low-glucose (1 g/L) DMEM (LG-DMEM, Cat# 31600034, ThermoFisher) containing 2% fetal bovine serum at 37 °C water bath for 30 minutes. The digestion was stopped by adding an equal volume of LG-DMEM containing 10% fetal bovine serum and 1 \times antibiotics (Antibiotic-Antimycotic, Cat# 15240096, ThermoFisher), namely, complete media (CM), and then centrifuged at 423 g for 10 minutes at room temperature. The fat-containing supernatant was discarded, and the cell pellet was washed twice with CM. Cells isolated from each mouse were then seeded into a 35-mm dish, cultured in CM, maintained in a 1 to 3 ratio, and passaged every 3 days when they reached 80% to 90% confluency.

Flow Cytometry Assay

MSCs at passage 3 were used for phenotypic characterization by flow cytometry. The MSCs were allowed to grow to 80% confluence and then trypsinized and suspended in PBS; 10⁶ cells were washed, resuspended in 100- μ L dyeing buffer, and incubated with FITC labeled CD45 (Cat# 103107), PE labeled CD34 (Cat# 152203) or CD105 (Cat# 120407), and APC labeled CD29 (Cat # 102215) antibodies, respectively. Isotype control immunoglobulin G labeled cells were used as control. All antibodies were purchased from Biolegend (San Diego, CA, US). The incubation was conducted at

room temperature for 30 minutes in the dark. The cells were washed twice with the dying buffer and analyzed by a Flow Cytometer (BD Biosciences, Franklin Lakes, NJ, US).

MSC Proliferation Assay

To evaluate the proliferation rate, 10^4 WT and *Tymp*^{-/-} MSCs were seeded into 24-well plates in triplicate and cultured in CM. Cells were trypsinized every other day and counted with a hemocytometer in combination with the Trypan Blue exclusion assay. In another set of experiments, WT and *Tymp*^{-/-} MSCs (10^3 /well) were seeded into 96-well plates with 8 replicates, and cell proliferation was assessed daily for up to 4 days using the MTT assay.^{29,36}

In another set of experiments, WT MSCs (3×10^3 /well) were seeded into 96-well plates and cultured in the CM overnight. The cells were then synchronized in serum-free LG-DMEM for 24 hours before they were stimulated with CM in the presence or absence of 10 μ M tipiracil or 25 ng/mL tumor necrosis factor- α (TNF- α) for the indicated times, and cell proliferation or viability was assessed by MTT assay.^{29,36}

To assess if TYMP affects the growth of MSCs under hypoxia or other low-nutrient conditions, WT and *Tymp*^{-/-} MSCs were seeded into a 12-well plate in a concentration of 2.8×10^4 /well and cultured overnight. The cells were then synchronized in serum-free LG-DMEM for 24 hours before they were stimulated with CM containing 150, 300, or 600 μ mol/L CoCl₂ for an additional 48 hours. Cell viability was then measured by the MTT assay.

Wound Healing Assay

WT and *Tymp*^{-/-} MSCs were seeded into 6-well plates at a density of 3.5×10^5 cells/well and cultured in the CM overnight. Cells were scratched with a 200- μ L pipette tip, rinsed with warm PBS 3 times, and images of the scratches were taken as the basal level of the “wound” (0 hours). The cells were then cultured under normal culture conditions, and images from the same places were taken again at the time points indicated in the results.²² Width of the scratch was measured using ImageJ (National Institutes of Health [NIH]), and the “wound” healing rate was calculated.²²

MSC Adhesion Assay

To assess MSC adhesive capability, a 96-well plate was coated with type I collagen, fibronectin, and bovine serum albumin (BSA) at a final concentration of 30, 10, and 10 μ g/mL in PBS, respectively. WT and *Tymp*^{-/-} MSCs were stained with Rhodamine 6G, and 10^3 cells were seeded into collagen/fibronectin/BSA mixture-coated wells and kept still in a cell incubator for 1 hour. The media was discarded, the unattached

cells were washed away with PBS, and cells attached to the bottom of the 96-well plate were randomly imaged and counted.

Cellix flow chambers were coated with type I collagen, fibronectin, and BSA at a final concentration of 30, 10, and 10 μ g/mL in PBS, respectively. MSCs in culture were trypsinized, collected, and resuspended in CM at a concentration of 10^5 cells/mL. Cells were stained with Rhodamine 6G at a final concentration of 50 μ g/mL and then perfused through the flow chamber at a flow rate of 10 μ L/min for 3 minutes. The chamber was washed with PBS at the same flow rate for 3 minutes to remove all nonattached cells, and all adhered cells were counted over the chamber. In some assays, the WT MSCs were pretreated with 50 μ M tipiracil for 5 minutes before they were used for the adhesion assay.

BM Cell Colony Formation

Mice were euthanized with an overdose of ketamine/xylazine, and femur bones were harvested under a sterilized condition. Soft tissues around the bone were removed, 2 ends of the femur bone were cut, and BM was isolated by flushing the femur bone cavity using 2 mL of PBS. To isolate nucleated cells, 2 mL Histopaque-077 solution was transferred to a 15-mL conical tube, and the 2 mL BM cells containing PBS were gently overlaid on top. The cells were then separated by centrifugation at 400 g for 30 minutes at room temperature. The top layer containing plasma was discarded and the opaque interface that contains mononuclear cells was transferred into a clean 15-mL conical centrifuge tube. Cells were washed 3 times with PBS, counted with Trypan blue, and 7×10^6 cells were seeded into a 35-mm dish and cultured in LG-DMEM containing 20% fetal bovine serum and antibiotics. Media were changed every 3 days, and crystal violet staining was conducted 15 days later to count the number of colony-forming units (CFUs). Areas covered by cell population ≥ 50 were analyzed using ImageJ.

In some experiments, to enhance stem cell mobilization, WT and *Tymp*^{-/-} mice were treated with CoCl₂ 10 mg/kg/day through intraperitoneal injection for 7 days, and AMD3100 5 mg/kg was given 1 day before sacrificing the mice.³⁷

Western Blot Assay

MSC lysates in RIPA buffer were prepared as described previously.^{26,27} Western blot assays were performed using antibodies against TYMP (SC-47702, Santa Cruz, CA), genes associated with retinoid-interferon-induced mortality-19 (GRIM-19) (Santa Cruz, sc-271 013), pan-AKT (#2920S), and Ser473-phospho-AKT (#4060S); all were from Cell Signaling (Danvers,

MA). Membranes were stripped and reblotted for pan-actin (#12748S) as a loading control.

Gelatin Zymography Matrix Metalloproteinase Activity Assay

MSCs (1.5×10^5 cells) were seeded into a 6-well plate, cultured for 24 hours, and allowed to reach $\approx 70\%$ confluency. Cells were washed with warm PBS 3 times and then cultured in serum-free LG-DMEM for an additional 24 hours. The cell culture media were collected and centrifuged at 423 g for 5 minutes to remove cell-related debris, and the supernatant was aliquoted and stored at -80°C for future use.

Gelatin zymography was conducted as mentioned in our previous studies.^{38–41} Briefly, 20 μL serum-free cell culture media were mixed with sample loading buffer (100 mmol/L Tris-HCl, pH 7.6, 4% SDS, 20% glycerol, and 0.004% Bromophenol Blue) in equal volume, incubated at 37°C for 30 minutes, and then dissolved in 7.5% SDS-PAGE containing 1 mg/mL gelatin (G9391-100G, Sigma-Aldrich). The gels were soaked in washing buffer (2.5% Triton X-100 in 0.05 M Tris-HCl, pH 7.5) with gentle shaking for 60 minutes with one change of the washing buffer at 30 minutes. The gels were rinsed with milli-Q water 2 times and then incubated in the incubation buffer (50 mmol/L Tris-HCl, pH 7.5, 5 mmol/L CaCl_2 , and 0.02% NaN_3) in a 37°C water bath overnight with gentle shaking (35 rpm). The gels were stained with GelCode Blue Stain Reagent (ThermoFisher) for 2 hours until clear bands were observed and then destained with water. Images were taken with FluoChem Imager.

Murine Cremaster Microthrombosis Model

Leukocytes and platelets were isolated from donor mice and labeled with CellTracker Green CMFDA and CellTracker Red CMTPIX (ThermoFisher), respectively. The fluorescently labeled leukocytes and platelets were washed with PBS to remove free dyes, mixed together, resuspended in 150 μL saline, and injected into male recipient mice through the jugular vein. TNF- α (500 ng in 100 μL saline) was then given to the recipient mice by injection, immediately after they received the injection of the leukocyte and platelet mixture. Three hours later, the cremaster muscle microcirculation model was prepared as described by Bagher and Segal.⁴² Microvessels were screened, and the formation of microthrombi was examined by intravital microscopy.^{27,43,44}

Statistical Analysis

Data were expressed as mean \pm SE. Data were analyzed for normality and equal variance using the

D'Agostino-Pearson normality test as a justification for using a 2-tailed Student *t*-test, Mann-Whitney test, or 1- or 2-way ANOVA for comparisons of 2 and >2 groups or factors. Repeated measures ANOVA or mixed effects 2-factor ANOVA were used for multiple time points and 2 factor comparisons. For the mixed-effects model, we treated genotype as the random effect and time as the fixed effect. For multiple hypothesis testing as shown in Table 1, we calculated the false discovery rate using the Benjamini-Hochberg method. GraphPad Prism (version 9.0.1) was used for data analysis and a $P \leq 0.05$ was considered statistically significant.

RESULTS

Deletion of TYMP in Mice Preserved Cardiac Function After AMI

Both AMI and ischemia/reperfusion mouse models are clinically relevant.^{45,46} To understand how TYMP affects myocardial function, cardiac remodeling, and healing after AMI, we induced AMI in mice by permanent ligation of the LAD.²⁹ Echocardiography was conducted to monitor cardiac function before surgery as well as 7 and 28 days after AMI (Figure 1A). As shown in Table 1, cardiac function evaluated by ejection fraction (EF) was similar between WT and *Tymp*^{-/-} mice before surgery. Cardiac function was decreased in both strains ($P=0.001$ and 0.005 in WT and *Tymp*^{-/-} versus their own basal levels, respectively) 7 days after LAD ligation. No significant difference was found 7 days after LAD ligation between WT and *Tymp*^{-/-} ($P=0.805$, Table 1). Cardiac function continually declined in the WT mice 28 days after surgery ($P=0.006$ versus day 7); however, it was preserved in the *Tymp*^{-/-} mice, and no further decline was found at 28 days when compared with 7 days after AMI ($P=0.07$). Cardiac function evaluated by fractional shortening showed a similar tendency as the EF (Table 1).

End-diastolic left ventricular internal diameter and end-systolic left ventricular internal diameter were significantly increased 28 days post-AMI compared with their preischemic values in both WT and *Tymp*^{-/-} hearts. However, the 2 groups were similar at all time points examined (Figure S1). Left ventricle anterior wall (LVAW) mass was also similar between the 2 groups although it slightly increased in both groups 28 days post-AMI (Table 1). LVAW, which is perfused by the LAD, was significantly thicker in the *Tymp*^{-/-} mice at the systolic phase on both 7 and 28 days after AMI (Table 1). Diastolic LVAW thickness was similar between groups. Interestingly, left ventricle posterior wall (LVPW) thickness showed an opposite phenotype, and LVPWd was significantly thicker in the WT mice. LVPWs was the same in the 2 groups at all the times examined. The DWS index is based on the linear elastic theory and is a useful simple

Table 1. Parameters Examined by Echocardiography

	Before surgery		1-week post-AMI		4-week post-AMI				
	WT (n=9)	<i>Tymp</i> ^{-/-} (n=9)	P value	WT (n=12)	<i>Tymp</i> ^{-/-} (n=10)	P value	WT (n=7)	<i>Tymp</i> ^{-/-} (n=12)	P value
Heart rate (beats/min)	343±6.687	341±6.2	0.87	316±7.7	300±13.45	0.3	289±9.75	294±9.07	0.7
EF	68.15±1.45	65.88±1.57	0.31	57.96±1.49*	57.35±2.00†	0.81	49.54±2.47*	62.85±2.15	0.001
FS%	37.68±1.14	35.85±1.17	0.28	30.11±1.01*	29.97±1.40†	0.93	24.99±1.50*	34.15±1.65	0.001
LV mass	112.99±7.06	120.48±10.08	0.54	105.57±8.10	110.11±6.40	0.67	130.82±12.67	140.05±11.83	0.61
LVAWd	0.84±0.047	0.86±0.05	0.71	0.81±0.07	0.83±0.027	0.83	0.81±0.03	0.95±0.057	0.065
LVAWs	1.48±0.078	1.29±0.062	0.09	1.11±0.054	1.27±0.031	0.03	1.10±0.075	1.53±0.064	0.001
LVPWd	0.95±0.055	1.06±0.118	0.39	1.0±0.07	0.88±0.053	0.2	1.03±0.076	0.82±0.041	0.021
LVPWs	1.28±0.093	1.25±0.087	0.77	1.28±0.069	1.25±0.033	0.71	1.22±0.138	1.27±0.074	0.72
DWS	0.25±0.027	0.16±0.048	0.11	0.2±0.06	0.3±0.037	0.22	0.14±0.045	0.33±0.061	0.035

AMI indicates acute myocardial infarction; DWS, diastolic wall strain; EF, ejection fraction; FS, fraction shortening; LV, left ventricle; LVAWd, left ventricle anterior wall thickness at diastolic phase; LVAWs, left ventricle anterior wall thickness at systolic phase; LVPWd, left ventricle posterior wall thickness at diastolic phase; LVPWs, left ventricle posterior wall thickness at systolic phase; and WT, wild-type. Diastolic wall strain was calculated using the equation: DWS=(LVPWs – LVPWd)/LVPWs. * and †, P<0.05 vs “Before surgery” in the same strain. Mixed-effects 2-factor ANOVA was used for the comparison of times and genotypes on the listed parameters, followed by multiple unpaired *t*-tests to identify the difference within each time point. Data are mean±SE. The false discovery rate was calculated using the Benjamini-Hochberg method. In this table, the raw P<0.05 threshold corresponds to a false discovery rate of 0.1575.

marker in assessing diastolic stiffness. While the DWS is similar in mice before and 7 days after LAD ligation, it is significantly smaller in the WT mice 28 days post-AMI (Table 1). These data suggest that although TYMP does not significantly affect cardiac dimension, TYMP deficiency reduced wall thinning of the infarcted myocardium and attenuated diastolic stiffness. This may have contributed to the improved cardiac function.

Evans blue and triphenyl tetrazolium chloride staining demonstrated that TYMP deficiency did not affect the size of AAR and infarct 18 hours after LAD ligation (Figure S2A through S2C); however, significantly reduced infarct sizes 4 weeks post-AMI (Figure 1B and 1C). These data suggest that the healing process of the *Tymp*^{-/-} myocardium may be enhanced.

TYMP Deficiency Increased Cardiac Perfusion But Paradoxically Attenuated Basal Contractility

To determine whether the increased EF in *Tymp*^{-/-} mice was due to *Tymp*^{-/-} hearts having enhanced contractility, we used Langendorff isolated hearts to evaluate cardiac function. TYMP deficiency did not affect heart rate (Figure 2A). Unexpectedly, the basal level coronary flow was slightly higher in the *Tymp*^{-/-} hearts (2.462±0.304 mL/min) than in the WT hearts (1.984±0.202 mL/min). LAD ligation reduced 24.2% of coronary flow in the WT hearts and 29.4% in the *Tymp*^{-/-} hearts. However, the coronary flow rate was still slightly higher in the *Tymp*^{-/-} hearts after LAD ligation (Figure 2B). Although there was no statistically significant difference, TYMP-deficient hearts generated lower developed pressure (Figure 2C) and smaller dP/dt (Figure 2D). Since increased cardiac contractility exacerbates cardiac function after AMI,^{47,48} these data suggest that TYMP deficiency-associated changes in the heart may increase its tolerance to ischemia and preserve cardiac function after AMI.

Deletion of TYMP in Mice Reduced Microthrombus Formation at the Acute Phase But Did Not Affect Angiogenesis, Apoptosis, and Inflammation in the Infarcted Hearts at the Chronic Phase

The contradiction of improved post-AMI EF and fractional shortening in *Tymp*^{-/-} hearts in vivo and a decreased contractility in the *Tymp*^{-/-} Langendorff hearts ex-vivo, lead us to consider that other parameters, such as perfusion to the hibernating myocardium or healing process, which includes inflammatory, proliferative, and healing phases,⁴⁹ may be enhanced due to TYMP deficiency. A greater basal coronary flow rate (Figure 2B) measured in the Langendorff hearts, a nonsignificant low AAR measured 18 hours after AMI (Figure S2B),

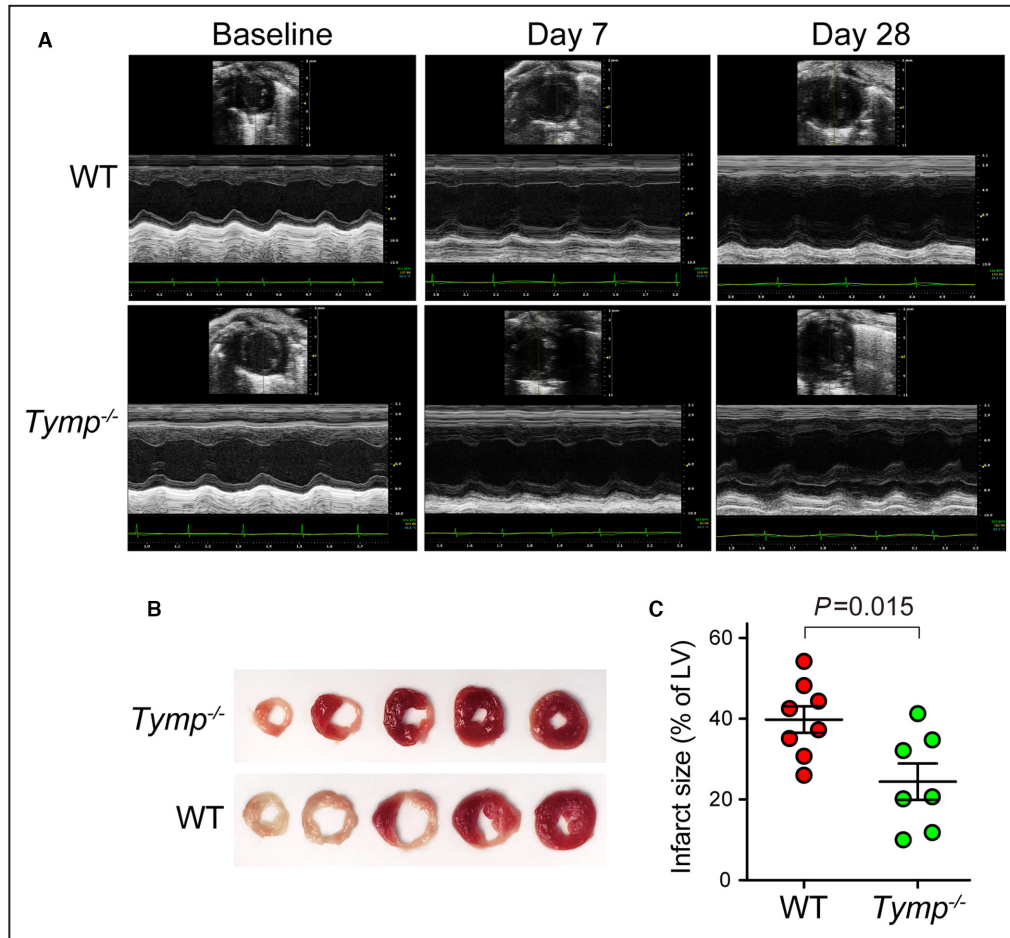


Figure 1. Thymidine phosphorylase deficiency in mice reduces infarct size and preserves cardiac function following left anterior descending coronary artery ligation.

Age-matched male wild-type C57BL/6J and thymidine phosphorylase knockout mice were subjected to the left anterior descending coronary artery ligation, a mouse model of acute myocardial infarction. **A**, Representative echocardiography images before left anterior descending coronary artery ligation, as well as 7 and 28 days after left anterior descending coronary artery ligation, were shown. **B** and **C**, Myocardial infarct size was assessed by triphenyl tetrazolium chloride staining 4 weeks after acute myocardial infarction. Infarct size was presented as the ratio of the area of infarction (pale) to the total area of the left ventricle. Data are expressed as mean \pm SE. Student *t*-test. LV indicates left ventricle; *Tymp*, thymidine phosphorylase; and WT, wild-type.

and a thicker systolic LVAW (Table 1) measured on 7- and 28-day post-AMI in the *Tymp*^{-/-} mice supports this speculation. Microthrombi formation in capillaries has been found in the myocardial ischemia/reperfusion model and it significantly reduces cardiac perfusion at the border zone.⁵⁰ By immunofluorescent staining for CD41, a platelet marker, we assessed the microthrombi density in hearts 24 hours after AMI using serial sections cut from the apex of the heart to the level of LAD ligation. Microthrombus was defined as an anuclear, CD41-positive structure in size about 10 to 30 μ m, which is much bigger than mouse platelets (\approx 0.5 μ m). We found significantly fewer microthrombi in the *Tymp*^{-/-} hearts than in the WT hearts (Figure 3A). Since TYMP deficiency did not affect the density of α -smooth muscle

actin-positive small arterioles examined 24 hours post-AMI (Figure S2D and S2E), we consider that the reduced microthrombi in the *Tymp*^{-/-} hearts contribute to the low AAR measured 18 hours after AMI. TYMP has proangiogenic and anti-apoptotic effects, we thus further evaluated vascular density and apoptosis in the hearts 4 weeks post-AMI. As shown in Figure 3B, TYMP deficiency did not affect angiogenesis evaluated by immunohistochemical staining for CD31 at both normal and ischemic zones. There was no cleaved caspase-3 detected (data not shown). However, the density of α -smooth muscle actin-positive arterioles was increased in the *Tymp*^{-/-} hearts (Figure 3C and 3D), suggesting that arteriogenesis may be enhanced during the healing phase in these mice.

Studies have indicated that TYMP may be pro-inflammatory as it is upregulated by several inflammatory cytokines including TNF- α , interleukin-1, interleukin-6, interleukin-8, interleukin-17, interferon- γ , and granulocyte-colony stimulating factor.^{20,51–53} By intrascrotal injection of TNF- α , we confirmed the high incidence of inflammatory microthrombus formation as well as the active interaction of leukocytes and platelets in the microcirculation of WT mice (Video S1). Since the sterile inflammatory phase after myocardial infarction is around 3 to 4 days in mice,^{49,54} we examined the expression of these cytokines in the infarcted myocardium 3 days post-AMI by quantitative polymerase chain reaction. As shown in Figure S3, TYMP

deficiency did not significantly affect the expression of the cytokines, chemokines, and other inflammation-related molecules examined.

TYMP Deficiency in Mice Enhanced BM Cell Mobilization After AMI

Adult cardiac myocytes are end-differentiated cells, which cannot be regenerated. Dead myocardium is replaced by scar tissue after injury. Earlier revascularization determines the fate of some myocardium that fell into ischemia but continue to survive. This is known as “hibernating myocardium.”⁵⁵ MSCs have become the essential adult cellular sources for regeneration medicine, including

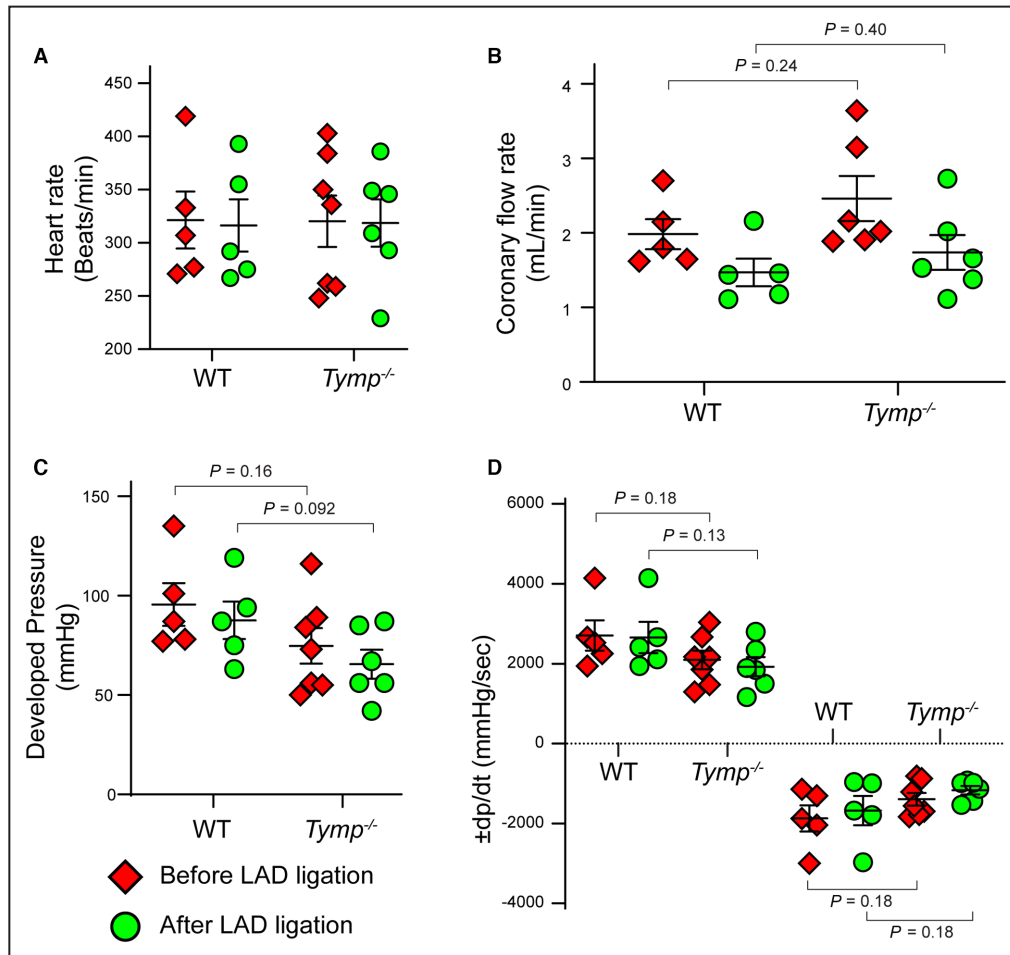


Figure 2. Thymidine phosphorylase deficiency tends to increase coronary artery flow but reduces cardiac contractility.

Hearts were isolated from age-matched female wild-type and thymidine phosphorylase knockout mice and rapidly mounted on a Langendorff isolated heart perfusion system. Hearts were allowed to acclimate for 15 minutes, and then parameters including heart rate (A), coronary flow rate (B), developed pressure (C), and \pm dp/dt (D) were recorded. The left anterior descending coronary artery was then ligated immediately below the first diagonal branch with an 8–0 suture. The hearts were perfused for an additional 10 minutes, and the above-mentioned parameters were recorded again. N=5 in the wild-type and N=6 in the thymidine phosphorylase knockout groups. All panels share the same legends shown below panel C. Data are expressed as mean \pm SE; 2-way ANOVA was used for statistical analyses followed by a Student *t*-test under each individual comparison between genotypes. LAD, left anterior descending coronary artery; *Tymp*, thymidine phosphorylase; and WT, wild-type.

therapies for the ischemic myocardium. However, some main problems including a low degree of retention of MSCs in the tissues, their short-lived viability after implantation, etc., remain unsolved.¹⁹ By using a skin ischemia model, Hamou et al reported that BM-derived MSCs were immediately mobilized, increased numbers in circulation and ischemic skin, and peaked around 7 days after injury.⁵⁶ Pula et al reported that TYMP enhances endothelial progenitor cell survival and it is highly expressed in CFU.⁵⁷ These studies suggest that TYMP may play a role in BM stem cell mobilization after AMI. To test this, we conducted a colony formation assay using BM cells harvested from mice 7 days post-AMI. As shown in Figure 4A, we found that TYMP deficiency dramatically enhanced CFU under this condition. To further confirm this finding, we treated WT and *Tymp*^{-/-} mice with CoCl₂ for 7 days to mimic hypoxia and AMD3100; a specific inhibitor of CXCR4, that tethers hematopoietic stem cells to the BM microenvironment, was given 1 day before sacrificing the mice to mobilize BM stem cells.^{37,58} BM was then harvested and used for colony formation assay. As shown in Figure 4B, CFU was identified from both strains and the numbers were significantly higher in the BM harvested from the *Tymp*^{-/-} mice under the chemically hypoxia-mimic condition. These data suggest that TYMP-deficient mice have a higher capability to mobilize BM stem cells under hypoxia. Since low numbers of CFU are correlated to increased cardiovascular risk,^{57,59} these data further suggest that TYMP deficiency generates an environment that enhances recovery of or preserves post-AMI cardiac function.

Deletion or Inhibition of TYMP in Mice Enhanced MSC Proliferation

In pathophysiological conditions, the source of MSCs that are responsible for repairing the damaged tissue could be either from the BM or from the original organ.⁶⁰ TYMP enhances endothelial cell chemotaxis but inhibits VSMC proliferation and migration,²⁰ suggesting that it acts differently in different cells. No study has examined the role of TYMP in MSCs. To determine whether TYMP affects MSC function, which results in a better cardioprotective effect, we cultured MSCs from white adipose tissue harvested from the perigonadal fat pad of male mice. Cell passages between 4 to 10 were used for the following studies and all comparisons were conducted using cells on the same passage.

The morphology of WT and *Tymp*^{-/-} MSCs was similar and expressed MSC markers (Figure S4). Interestingly, we found that, during culture, TYMP-deficient MSCs grew faster than WT MSCs. To confirm this finding, cells were seeded at a concentration of 10⁴ cells/well into 24-well plates, trypsinized, and counted using the Trypan Blue Exclusion Assay every other day. As shown in Figure 5A, TYMP deficiency dramatically increased

the proliferation rate of the MSCs. This finding was confirmed by MTT assay (Figure 5B). Tipiracil inhibits TYMP function with an IC₅₀ at 34 nmol/L.²⁷ In line with TYMP deficiency, treating WT MSCs with tipiracil significantly enhanced WT MSC proliferation (Figure 5C). These data suggest that TYMP deficiency or inhibition with its selective inhibitor enhances MSC proliferation, which may contribute to the cardioprotective effects found in the *Tymp*^{-/-} mice, in addition to the reduced microthrombosis and the enhanced arteriogenesis.

Deletion of TYMP Enhances MSC Homing Capability

Efficient homing and migration of MSCs toward lesion sites are critical in achieving a therapeutic effect.⁶¹ To determine whether TYMP affects MSCs migration and homing, we first conducted a wound healing assay using WT and *Tymp*^{-/-} MSCs.²² As shown in Figure 6A, TYMP deficiency in MSCs significantly shortened the time to cover the “wounded” area. It took 24 hours for the WT MSCs to reach a similar level of “wound healing” found in the *Tymp*^{-/-} mice at 18 hours. This piece of data suggests that TYMP-null MSCs may have higher mobility to home to the lesion site. To test this hypothesis, WT and *Tymp*^{-/-} MSCs were stained with Rhodamine 6G, seeded into collagen/fibronectin/BSA mixture-coated 96-well plates in a concentration of 10³ cells/well, and kept still in the cell incubator for 1 hour. The culture media were discarded and unattached cells were washed away with PBS. Cells attached to the bottom of the 96-well plate were randomly imaged. As shown in Figure 6B, the average cell density per field (×20 magnification) was significantly higher in the *Tymp*^{-/-} MSCs. By analyzing images shown in Figure 6B, we noticed that *Tymp*^{-/-} MSCs were likely larger than WT cells. To confirm this finding, we randomly involved 14 images from the WT and 5 images from the *Tymp*^{-/-} group and measured the size of all MSCs attached to the dish. Total of 140 WT and 229 *Tymp*^{-/-} MSCs were found in these images. The average cell size in the 2 groups was similar (0.262±0.0096 in WT versus 0.268±0.0098 in *Tymp*^{-/-}, *P*=0.68). However, as shown in Figure 6C, the percentage of larger cells was higher in the *Tymp*^{-/-} group. To further determine the adhesiveness of the MSCs under a flow condition, we conducted a Cellix flow chamber assay and tested the capability of WT and *Tymp*^{-/-} MSCs' binding to the extracellular matrix-coated surface under a capillary flow rate of 10 μL/min.⁶² As shown in Figure 6D and Video S2 (WT) and (*Tymp*^{-/-}), TYMP deficiency significantly increased MSC adhesion to the collagen/fibronectin/BSA mixture-coated surface. These data suggest that TYMP deficiency in MSCs enhances their capability of mobilization and adhesion, which may promote their homing to the injury sites.

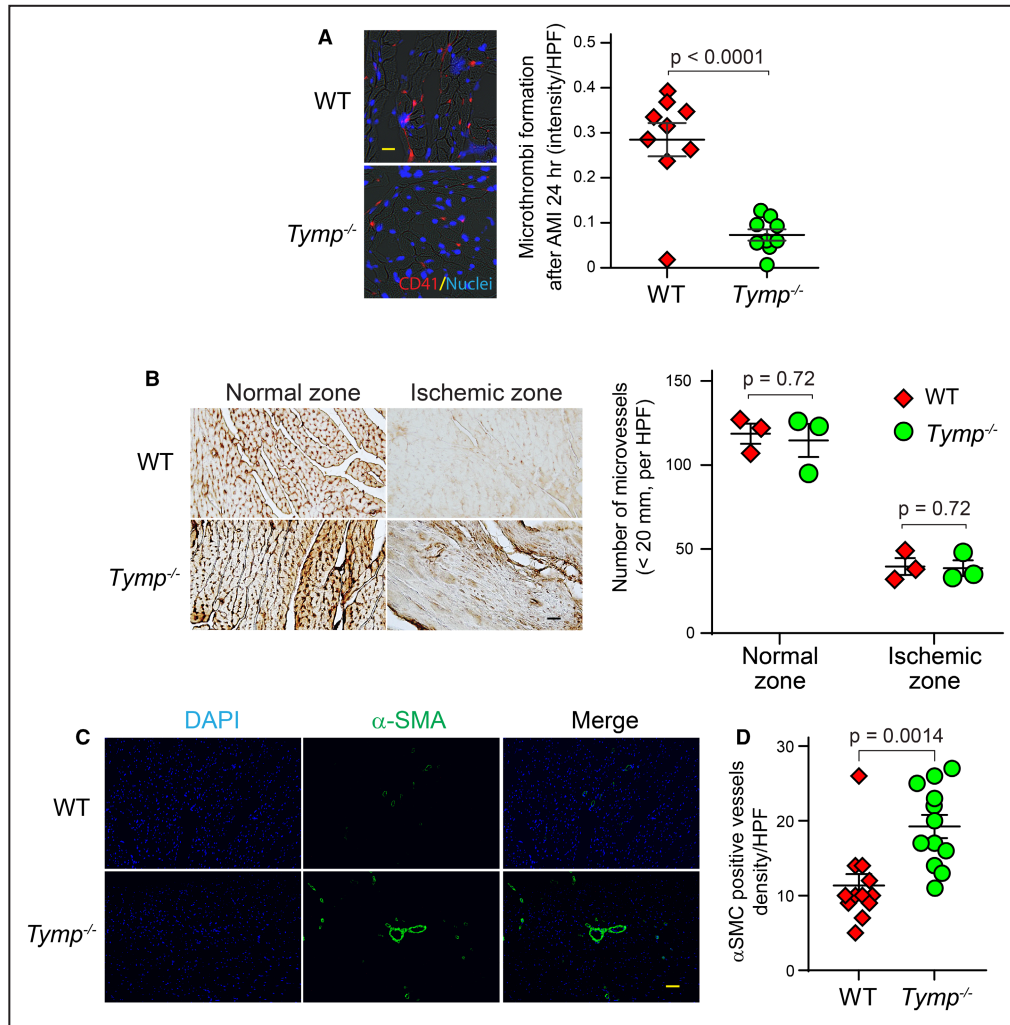


Figure 3. Thymidine phosphorylase deficiency in mice reduces microthrombus formation after acute myocardial infarction and enhances arteriogenesis.

A, Mice were euthanized 24 hours after left anterior descending coronary artery ligation. The hearts were removed and frozen. Frozen hearts were cross-sectioned from the apex to the level of the left anterior descending coronary artery ligation. Three sections at similar levels were randomly selected from each mouse and stained for CD41 (red), a platelet marker. Nuclei were stained with DAPI. Microthrombi were defined as anuclear structures between 10 to 30 μ m in size. One image was randomly taken from each section, and red fluorescence intensity was analyzed using ImageJ. The scatter plot represents accumulated data from 3 mice, 3 sections from each mouse. Student *t*-test; $n=9$. Scale bar=30 μ m. **B**, Hearts harvested 4 weeks after acute myocardial infarction were embedded in paraffin and sectioned. Immunohistochemical staining was conducted for CD31. Two-way repeated measures ANOVA was used for statistical analyses followed by a Student *t*-test under each individual comparison between genotypes. Scale bar=50 μ m. **C**, Immunofluorescence staining was conducted for α -smooth muscle actin, and images at the border zones of each heart were obtained. Scale bar=50 μ m. **D**, The number of α -smooth muscle actin positive vessels from 4 mice; 3 randomly selected regions from each mouse were counted and compared between the 2 groups. Student *t*-test; $n=12$. α -SMA indicates α -smooth muscle actin; DAPI, 4',6-diamidino-2-phenylindole; *Tymp*, thymidine phosphorylase; and WT, wild-type.

TYMP-Deficient MSCs Are Tolerant to Hypoxic and Low-Nutrient Conditions

Infarcted or ischemic myocardium is deprived of nutrition and oxygen supplies. To determine whether TYMP deficiency-enhanced proliferation, mobilization, and homing capability of MSCs benefit cardiac recovery

under these severe conditions, we treated WT and *Tymp*^{-/-} MSCs with CoCl₂ to mimic the hypoxic condition.^{22,29} Unexpectedly, in comparison with untreated control cells, both WT and *Tymp*^{-/-} MSCs showed increased proliferation in response to 150 and 300 μ M CoCl₂ treatment for 24 hours (Figure 7A). Treating

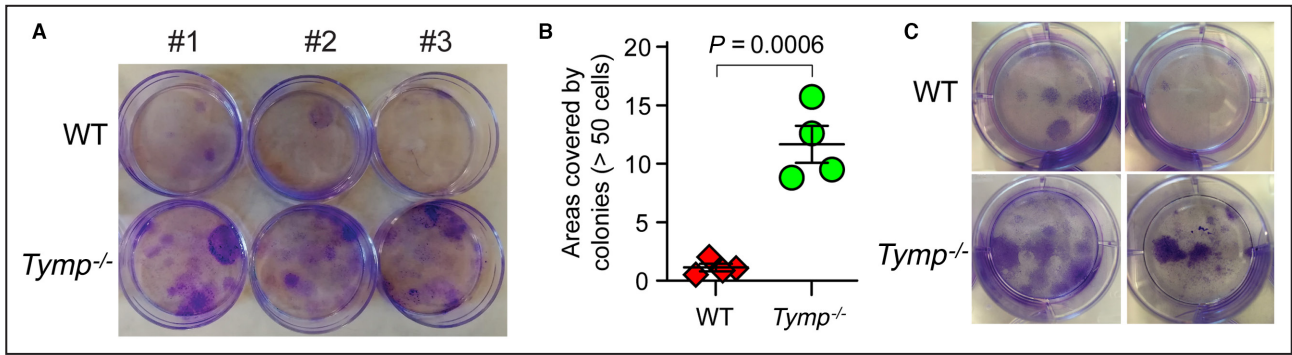


Figure 4. Thymidine phosphorylase deficiency enhances bone marrow cell-derived colony formation.

A, Colony formation assay was conducted using bone marrow cells harvested from mice 7 days post-acute myocardial infarction. Three technical repeats are shown. **B**, Quantitative analyses of areas covered by colonies. Student *t*-test. **C**, Colony formation assay using bone marrow cells harvested from mice treated with CoCl₂/AMD3100. *Tymp* indicates thymidine phosphorylase; and WT, wild-type.

MSCs with 600 μM CoCl₂ killed ≈75% of WT MSCs; however, it did not significantly affect the viability of *Tymp*^{-/-} MSCs. These data suggest TYMP-deficient MSCs possess a characteristic that provides resistance to the severe hypoxia and low-nutrient conditions,

much like the microenvironment of an infarction zone. Since inflammation is increased post-AMI,⁶³ we further determined how WT and *Tymp*^{-/-} MSCs respond to a proinflammatory environment by testing their response to TNF-α treatment in vitro. As shown in Figure 7B,

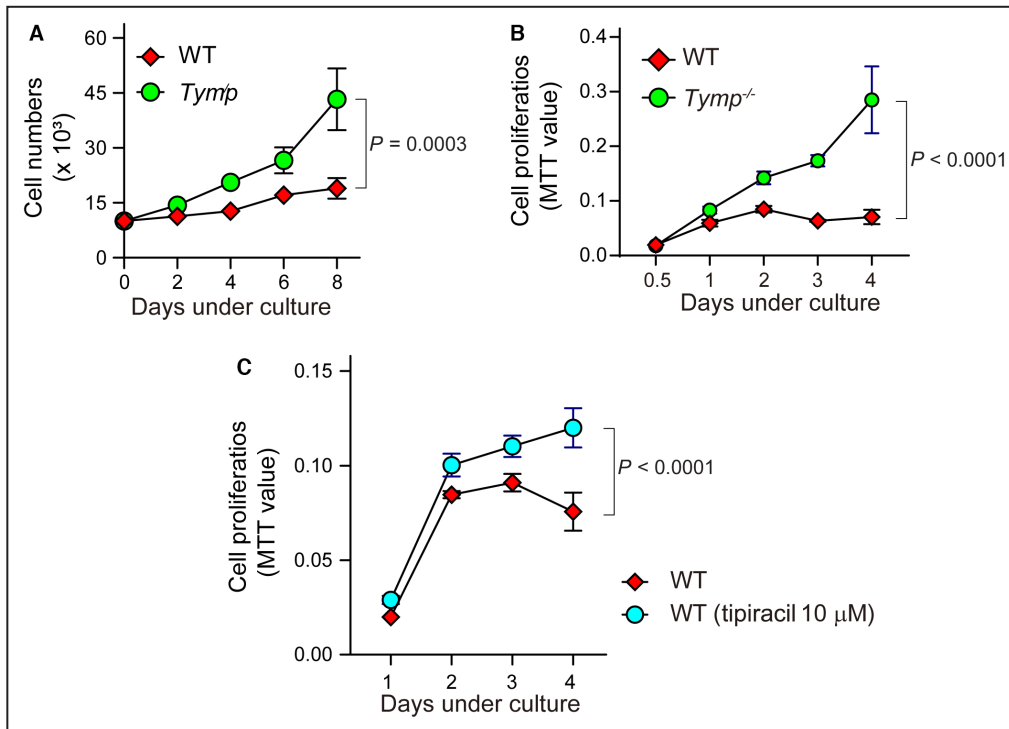


Figure 5. Thymidine phosphorylase deficiency in mice enhanced the proliferation of mesenchymal stem cells.

A, Mesenchymal stem cells were seeded into 24-well plates in a concentration of 10⁴ cells/well and counted every other day. N=3 at each time point. **B**, Wild-type and thymidine phosphorylase knockout mesenchymal stem cells (10³/well) were seeded into 96-well plates, and cell proliferation was assessed daily for up to 4 days using the MTT assay. N=8 at each time point. **C**, Wild-type mesenchymal stem cells (3×10³/well) were seeded into 96-well plates, synchronized for 24 hours, and cultured in normal culture conditions in the presence or absence of 10 μM tipiracil. Cell proliferation was assessed using the MTT assay at the indicated time points. N=8 at each time point. Mixed-effects 2-factor ANOVA was used to determine the difference between wild-type and thymidine phosphorylase knockout. MTT indicates 3-(4,5-dimethylthiazol-2-yl)-2,5-diphenyltetrazolium bromide; *Tymp*, thymidine phosphorylase; and WT, wild-type.

treating MSCs with 25 ng/mL TNF- α almost blocked the growth of WT but had less effect on the *Tymp*^{-/-} MSCs. To assess the response of WT and *Tymp*^{-/-} MSCs in the ischemic environment in vivo, we stained WT MSCs with CellTracker Green and *Tymp*^{-/-} MSCs with CellTracker Red, mixed equal amounts of each type (Figure S5), and then injected the mixture into the border zone of the infarcted myocardium. Mice were euthanized on days 1 and 3 postinjection and hearts were sectioned. As shown in Figure 7C, both cells were clearly seen in mice 24 hours after intramyocardial injection (top panel, close to left ventricle). However,

fewer green MSCs were seen compared with red MSCs after 72 hours, suggesting that more *Tymp*^{-/-} MSCs survived or were retained in the injection site.

We previously found that TYMP is positively correlated with matrix metalloproteinase-2 and -9 (MMP2 and MMP9) activation and expression in canine hearts.^{38,39} Since MMP2 plays an important role in MSC extravasation,⁶⁴ we examined MMP2 and MMP9 activity in MSCs-conditioned media by gelatin zymography as well as mRNA expression in the infarcted hearts by quantitative polymerase chain reaction. There was no detectable MMP9 activity in the MSC culture media.

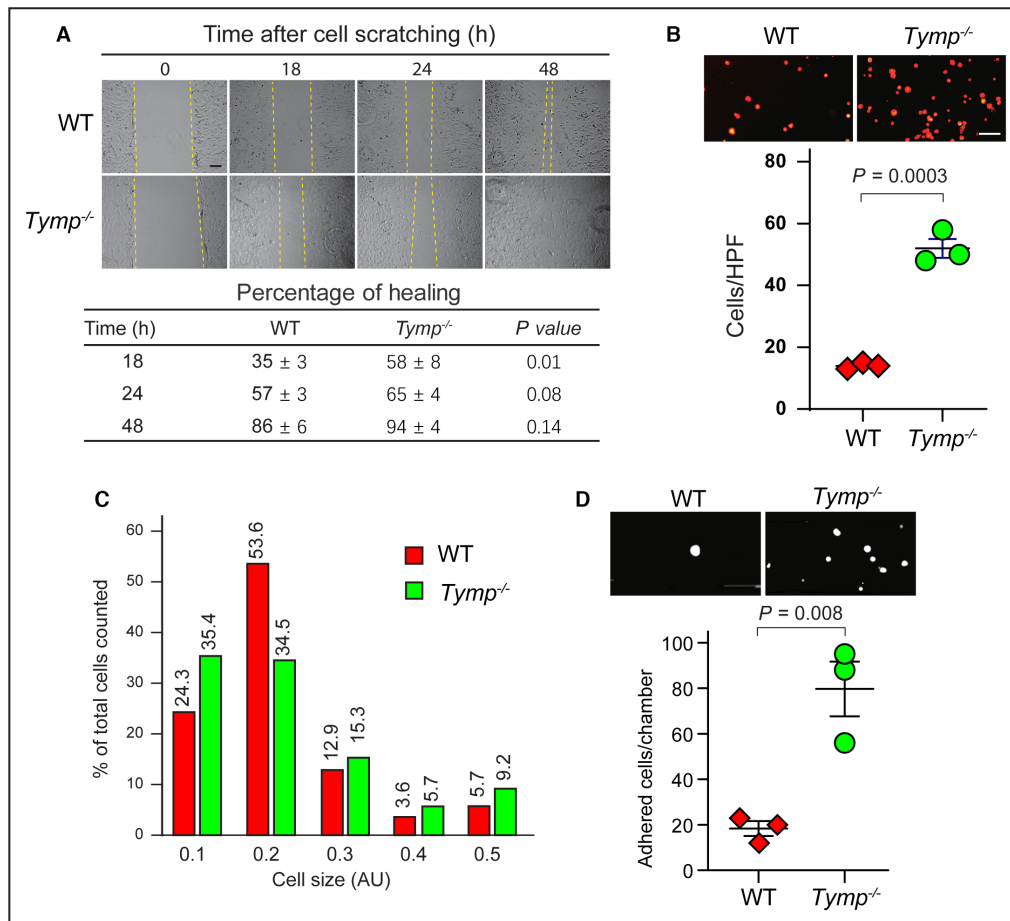


Figure 6. Thymidine phosphorylase deficiency enhanced mesenchymal stem cells homing capability.

A, Wild-type and thymidine phosphorylase knockout mesenchymal stem cells (MSCs) were seeded into 6-well plates at a density of 3.5×10^5 cells/well and cultured in normal culture media overnight. Cells were scratched with a 200 μ L pipette tip, rinsed with warm PBS, and images of the scratches were obtained at the indicated time points. The percentage of healing (areas covered by cells) was analyzed by ImageJ. Student *t*-test; *n*=6 at each time point. Scale bar=150 μ m. **B**, Wild-type and thymidine phosphorylase knockout MSCs were stained with Rhodamine 6G and seeded into collagen/fibronectin/BSA mixture-coated 96-well plate for 1 hour. Unattached cells were washed away and cells adhered to the well bottom were counted. Scale bar=20 μ m. Student *t*-test; *n*=3. **C**, Size (arbitrary unit, AU) of wild-type and thymidine phosphorylase knockout MSCs used for adhesion assay as mentioned in (B) were analyzed with ImageJ, and the percentage at each size was calculated. **D**, Cellix flow chamber coated with collagen/fibronectin/BSA mixture was used to test the adhesion capability of MSCs under a capillary flow rate of 10 μ L/min. The scatter plot shows the total cell counts in each chamber. Student *t*-test; *n*=3. *Tymp* indicates thymidine phosphorylase; HPF, high-power field, and WT, wild-type.

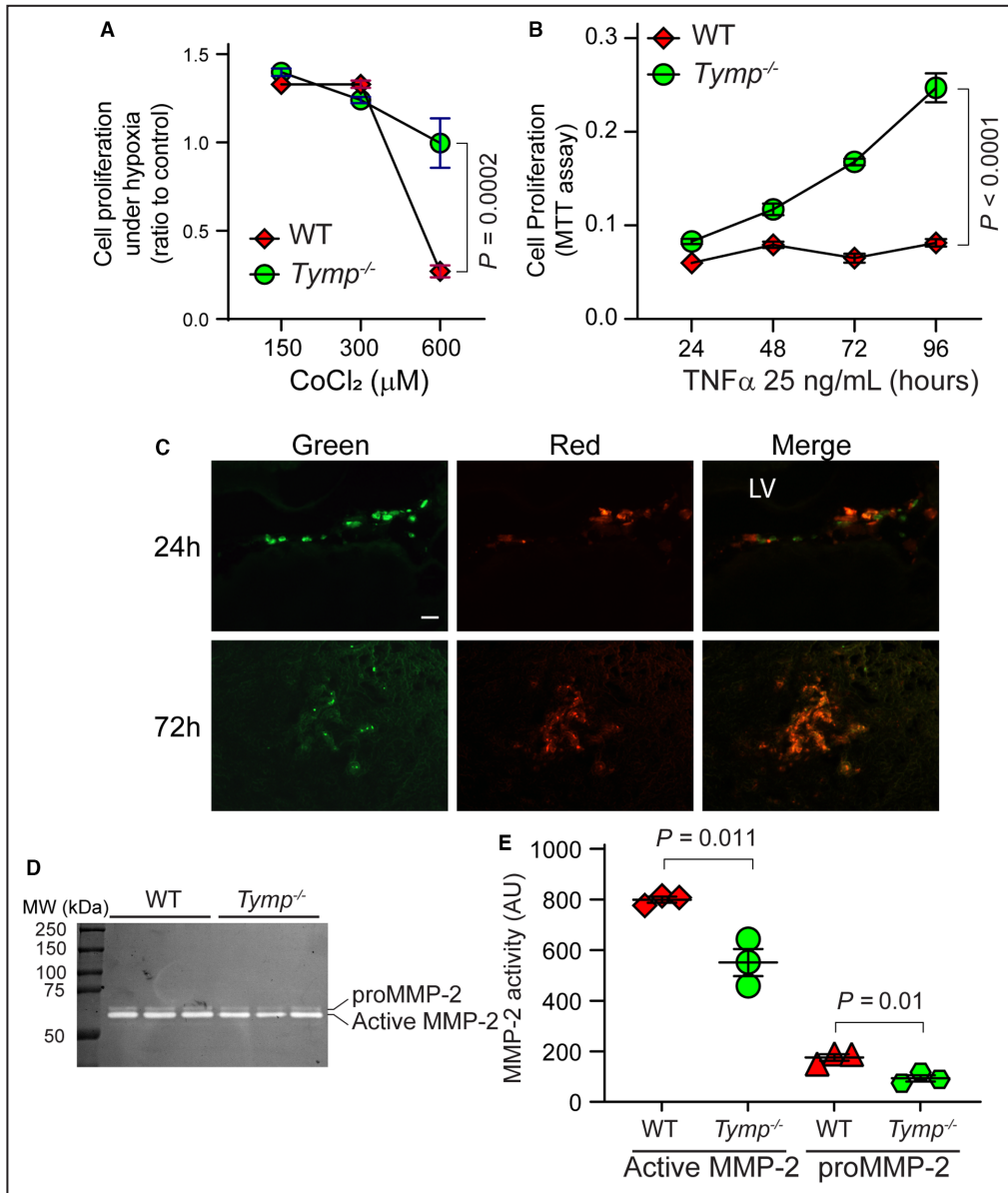


Figure 7. Thymidine phosphorylase-deficient mesenchymal stem cells are tolerant to hypoxic and low-nutrient conditions.

A, Wild-type and thymidine phosphorylase knockout mesenchymal stem cells were seeded into a 12-well plate at a density of 2.8×10^4 cells/well and cultured in normal culture media overnight. Cells were then synchronized in serum-free low-glucose DMEM for 24 hours and restimulated with normal culture media containing different concentrations of CoCl_2 . Cell viability was measured 48 hours later by the MTT assay. Mixed-effects 2-factor ANOVA; $n=4$. **B**, Wild type and thymidine phosphorylase knockout mesenchymal stem cells (3×10^3 /well) were seeded into a 96-well plate and cultured under normal conditions overnight. Cells were synchronized in serum-free low-glucose DMEM for 24 hours and recultured in normal media containing tumor necrosis factor- α (25 ng/mL) for the indicated times. Cell viability was assessed with the MTT assay. Mixed-effects 2-factor ANOVA; $n=8$ at each time point. **C**, Wild type and thymidine phosphorylase knockout mesenchymal stem cells were stained with cell tracker green and red, respectively. The same number of cells was mixed together and injected into the border zone of wild-type acute myocardial infarction hearts. Hearts were taken 24 or 72 hours later, sectioned, and the cells retained in the infarct myocardium were examined. Scale bar=100 μm . **D**, Gelatin zymography. Wildtype and thymidine phosphorylase knockout mesenchymal stem cells (1.5×10^5) were seeded into a 6-well plate and cultured overnight. Cells were washed with warm PBS and then cultured in serum-free media for an additional 24 hours. The serum-free media was subjected to gelatin zymography to measure matrix metalloproteinase-2 and -9 activity. **E**, Statistical analysis of matrix metalloproteinase-2 band intensity analyzed with ImageJ. Student *t*-test; $n=3$. MMP-2 indicates matrix metalloproteinase-2; MTT, 3-(4,5-dimethylthiazol-2-yl)-2,5-diphenyltetrazolium bromide; TNF- α , tumor necrosis factor-alpha; Tymp, thymidine phosphorylase; and WT, wild-type.

However, MMP2 activity was significantly reduced in the *Tymp*^{-/-} MSCs-conditioned culture media compared with the media of WT MSCs (Figure 7D and 7E). No MMP9 was detectable in the infarcted hearts by polymerase chain reaction. MMP2 was detectable. However, there was no statistical difference between the 2 groups (data not shown).

Deletion of TYMP Reduced GRIM-19 Expression But Enhanced AKT Activity in MSCs

GRIM-19 is an assembling subunit of the mitochondrial complex I and has a significant effect on energy production. However, as it is named, GRIM-19 also mediates interferon-induced cell death.⁶⁵ GRIM-19 expression, assessed by western blot (Figure 8A and B), was lower in *Tymp*^{-/-} MSCs than in WT cells. Our previous studies have demonstrated that TYMP plays a role in regulating AKT phosphorylation.^{24,26,27} Unexpectedly, we found phosphorylated AKT was significantly increased in the *Tymp*^{-/-} MSCs under normal culture conditions (Figure 8A and 8C).

Tipiracil Treatment Improved Cardiac Function After AMI

Tipiracil is a US Food and Drug Administration-approved drug. To test the potential translational relevance of our novel findings described above, we examined the effect of tipiracil on AMI. As shown in Table 2, tipiracil treatment mimicked the phenotype of TYMP deficiency and significantly preserved cardiac function, reduced anterior wall thinning, and attenuated diastolic stiffness of WT mice examined 4 weeks after AMI. Tipiracil treatment also significantly reduced infarct size (Figure 9).

DISCUSSION

In this study, we found that deletion of TYMP in mice significantly preserved cardiac function post-AMI. The potential mechanisms that mediate this cardioprotection include: (1) TYMP deficiency reduces microthrombi formation in the ischemic myocardium, which may improve blood perfusion to the border zone “hibernating myocardium” and reduce infarct size. (2) TYMP deficiency enhances BM stem cell mobilization, which may enhance the healing process. (3) TYMP deficiency leads to the generation of “powerful” MSCs that have enhanced proliferation, migration, and adhesion as well as resistance to hypoxia and inflammation-associated death. These characteristics may enhance MSCs homing to lesion areas post-AMI.

The fate of the infarcted myocardium depends on several factors including the abundance of collateral circulation, the severity of local inflammation, and microthrombus formation, as well as fibrinolytic activity.^{66,67} Enhanced angiogenesis has been known to play important roles in rescuing the stunned myocardium post-AMI.^{68,69} It is well documented that TYMP has a proangiogenic effect,^{20,57} and we previously demonstrated that delivery of a TYMP-encoding plasmid into infarcted canine myocardium significantly improved cardiac function and regional blood perfusion.^{4,21,70} Here we found that TYMP deficiency did not affect angiogenesis (by evaluation of CD31-positive vessels) in either normal or infarcted myocardium (Figure 3B). TYMP global-deficient mice have normal fertility, growth, size, and lifespan, suggesting that the TYMP-mediated proangiogenic effect is not essential for the development, although it is correlated with angiogenesis under some disease conditions, such as cancer.^{71,72}

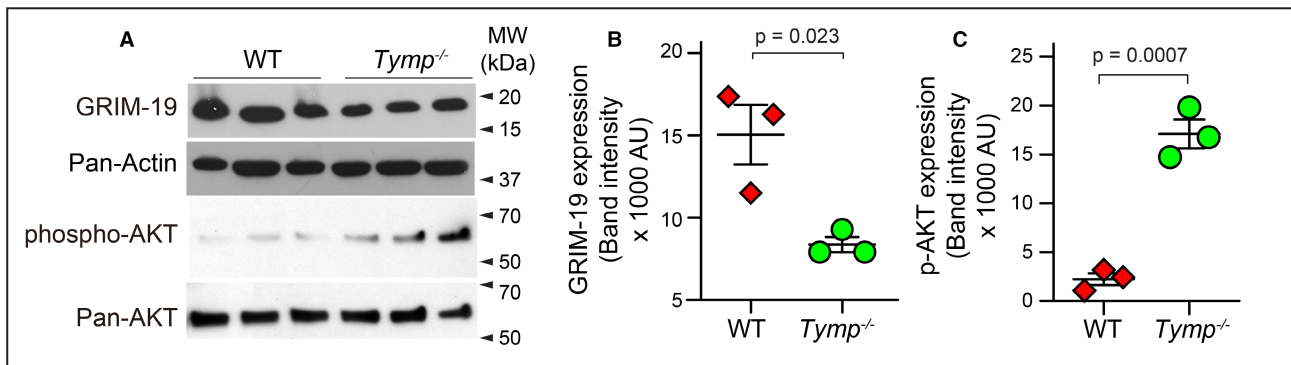


Figure 8. Thymidine phosphorylase deficiency reduced expression of GRIM-19 but induced constitutive activation of AKT in mesenchymal stem cells.

A, Wild-type and thymidine phosphorylase knockout mesenchymal stem cells cultured under normal passaging conditions were grown for 3 days, at roughly 80% to 90% confluence. The cells were harvested and lysed in radioimmunoprecipitation assay buffer. Western blot assays were conducted using antibodies against the indicated molecules. Each lane represents cells cultured from different patches. Blots represent 3 biological repeats. **B** and **C**, the intensity of western blot bands shown in **A** were analyzed with ImageJ. Student *t*-test; *n*=3. GRIM-19 indicates genes associated with retinoid-interferon-induced mortality-19; *Tymp*, thymidine phosphorylase; WT, wild-type; and MW, molecular weight.

Table 2. Parameters Examined by Echocardiography

	4-week post-AMI		
	WT	WT+Tipiracil	P value
Heart rate (beats/min)	289±9.75	274±20	0.36
EF	49.54±2.47*	67.07±0.25	0.0005
FS%	24.99±1.50*	36.9±0.37	0.0003
LV mass	130.82±12.67	122.47±10.58	0.667
LVAWd	0.81±0.03	0.86±0.081	0.452
LVAWs	1.10±0.075	1.37±0.046	0.034
LVPWd	1.03±0.076	0.9±0.074	0.307
LVPWs	1.22±0.138	1.29±0.093	0.747
DWS	0.14±0.045	0.30±0.025	0.032

AMI indicates acute myocardial infarction; DWS, diastolic wall strain; EF, ejection fraction; FS, fraction shortening; LV, left ventricle; LVAWd, left ventricle anterior wall thickness at diastolic phase; LVAWs, left ventricle anterior wall thickness at systolic phase; LVPWd, left ventricle posterior wall thickness at diastolic phase; LVPWs, left ventricle posterior wall thickness at systolic phase; and WT, wild-type. Diastolic wall strain is calculated using the equation: $DWS = (LVPWs - LVPWd) / LVPWs$. N=4 in wild-type+tipiracil treated, 7 in the wild-type group. Student *t*-test was used.

Our previous studies demonstrated that TYMP deficiency reduced platelet activation in response to common agonists such as collagen, ADP, and thrombin, and inhibited thrombosis in the ferric chloride ($FeCl_3$)-injured carotid artery.^{26,27} For the first time, to our knowledge, we found that TYMP deficiency also significantly attenuated microthrombi formation in the myocardium examined 24 hours after LAD ligation. Microthrombi formed in the infarct-related arteries of the myocardium affect the regional perfusion and functional recovery of viable myocardium. This subsequently affects the infarct size and the healing process.⁷³ Thus, although AAR and infarct size are the same in WT and *Tymp*^{-/-} mice in the early phase, we believe that the TYMP deficiency-associated reduction of microthrombi contributed to the reduced infarct size and the preserved cardiac function in the chronic phase.

The role of inflammation post-AMI is controversial. Inflammation plays an important role in attracting various cells including neutrophils, monocytes, and macrophages to the infarct area to remove necrotic cell debris.⁷⁴ Microthrombi formed in the infarcted myocardium may also play an important role in inflammation, and the release of various cytokines from the clotted platelets can attract additional leukocytes to the infarct zone.⁷⁵ These infiltrated leukocytes further exacerbate inflammation resulting in enlargement of the ischemic injury beyond the original infarction zone. In addition, the increased regional inflammation may also cause an imbalance between the procoagulant and anticoagulant systems,⁷⁶ leading to additional microthrombi formation as shown in the Video S1. Although we did not find that TYMP deficiency significantly affected the expression of cytokines, chemokines, or TLRs, at the mRNA level, we believe that TYMP deficiency breaks or attenuates the positive feedback loop between microthrombi and inflammation, which may contribute to

the preserved cardiac function. The attenuated microthrombi also improve regional blood circulation, which can enhance the clearance of leukocytes.

MSCs usually exist in an environment with oxygen concentration between 2% to 9%.⁷⁷ This may explain why they had an increased proliferation under low $CoCl_2$ treatment (Figure 7A). We have reported that TYMP inhibits VSMC proliferation.²² Here we found that TYMP also inhibits MSC proliferation, and TYMP deficiency not only enhances MSC proliferation under normal culture conditions but also increases MSC survival in the milieu of hypoxia and inflammation. These characteristics may render TYMP-deficient MSCs more capable of repairing infarcted myocardium. Studies have shown various retention rates of MSCs after administration in a range of 1.7% to 13.74%.⁷⁸ However, because of the time examined, animal models used, and different cell sources in each individual study, the dynamic changes of MSC after administration in each study cannot be simply compared. By regional injection of cell-tracker labeled WT and *Tymp*^{-/-} MSCs mixture, we found that both cells were present at the injury sites 24 hours after injection. However, WT cells were significantly reduced 72 hours later. In addition to that *Tymp*^{-/-} MSCs are resistant to hypoxic and inflammatory conditions, their increased size, increased adhesion to the extracellular matrix, and decreased MMP2 expression may also contribute to their retention in the injury site. Campbell and colleagues have reported that cell size is critical for the initial retention,⁷⁹ and both active adhesion and passive arrest mediate MSC extravasation.⁶¹ Under a high shear flow rate, TYMP has no effect on adhesion (data not shown). However, under a microvascular flow rate as shown in Figure 6D, TYMP deficiency significantly increased MSC adhesion. These data suggest that TYMP-deficient MSCs

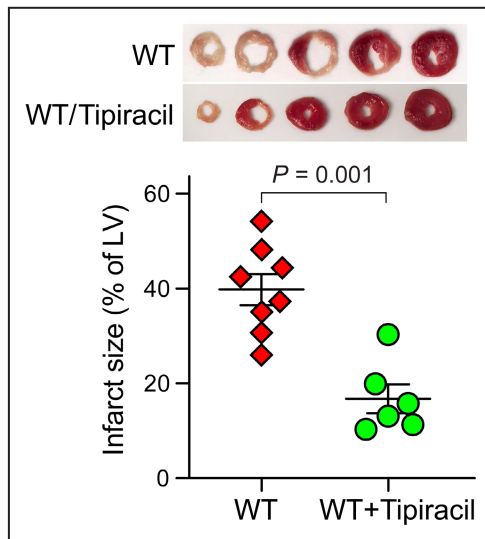


Figure 9. Tipiracil treatment preserves cardiac function and reduces infarct size.

Wild-type mice were pretreated with tipiracil (1 mg/kg) by oral administration for 1 week and then subjected to ligation of the left anterior descending coronary artery. Mice continually received tipiracil (1 mg/kg) for 28 days after acute myocardial infarction. Triphenyl tetrazolium chloride-based infarct size was compared with wild-type mice shown in Figure 1B and 1C. Student *t*-test. LV indicates left ventricle; and WT, wild-type.

may have an enhanced homing capability. In line with our previous studies in which we found that TYMP is positively associated with MMP2 and -9 activities,³⁸ here we found that TYMP deficiency reduced MMP2 activity in MSC-conditioned culture media (Figure 7D and 7E). The reduced MMP2 activity may also contribute to MSC retention. A study by Vincent and colleagues demonstrated that MSCs migrate toward stiffer fragments.⁸⁰ Uncontrolled MMPs degrade ECM proteins and thus reduce external rigidity.⁸¹

We have found that ADP-stimulated AKT phosphorylation in platelets showed 2 phases.^{26,27} In the first phase, TYMP deficiency slightly increased AKT phosphorylation. However, AKT activation was significantly decreased in the second phase.²⁷ In this study, unexpectedly, we found that TYMP deficiency induced a constitutive AKT phosphorylation in MSCs. While we still do not know the detailed mechanism behind this change, AKT signaling has been known to play an important role in cell penetration and survival.^{82,83} Interestingly, Seung and colleagues recently found that ADP receptor P2Y₁₂-dependent signaling is involved in emergency hematopoiesis after AMI and enhances post-AMI cardiac injury.⁸⁴ It would be important to determine if TYMP is involved in P2Y₁₂-mediated emergency hematopoiesis. Furthermore, we found that TYMP deficiency also significantly reduced the expression of GRIM-19, a proapoptotic protein. The reduced GRIM-19 expression may also

contribute to the MSC homing. Hwang et al. reported that GRIM-19 was weakly expressed in the hippocampal subgranular zone, where neural stem and progenitor cells are abundant. However, GRIM-19 is highly expressed in the immature and mature neuronal cells in the granular cell layer of the normal brain, suggesting that an inverse correlation is present between the expression of GRIM-19 and stemness activity.⁸⁵ These findings provide additional mechanistic evidence that TYMP deficiency or inhibition leads to MSC character changes, which promote MSC proliferation, migration, and retention in the injury zone, and thus enhance the healing process of the injured myocardium.

Our data reveal that TYMP deficiency generates an environment that preserves or improves cardiac function after AMI. TYMP-deficient mice not only have improved EF, fractional shortening, and thicker systolic LVAW but also have better left ventricle compliance (eg, increased DWS). Recent guidelines for echocardiography in experimental mice^{46,86} suggest that the use of ketamine/xylazine during echocardiography might be a limitation of this study. However, the comparison of these parameters of cardiac function between the 2 groups should not be affected by anesthesia since all data were acquired at similar heart rates as shown in Tables 1 and 2.

In conclusion, this study demonstrated for the first time that TYMP deficiency or inhibition significantly preserved cardiac function following AMI in mice. TYMP deficiency or inhibition may not only attenuate ischemic myocardium against injury in the early phase by reducing microthrombosis but also enhances MSC function, which enhances the healing process post-AMI. TYMP could be a novel target for the treatment of AMI.

ARTICLE INFORMATION

Received August 31, 2022; accepted February 22, 2023.

Affiliations

Department of Biomedical Sciences, Joan C. Edwards School of Medicine at Marshall University, Huntington, WV (L.D., H.Y., B.R.R., O.Q.Y.L., A.R.D., G.T.-A., L.H., J.D., W.L.); Department of Pathophysiology, College of Basic Medical Science, China Medical University, Shenyang, Liaoning, China (L.D.); Department of Pharmaceutical Sciences, School of Pharmacy at Marshall University, Huntington, WV (B.R.R.); and Department of Medicine, Joan C. Edwards School of Medicine at Marshall University, Huntington, WV (E.T.).

Sources of Funding

This work is supported by the Marshall University Institute Fund (Start fund to Wei Li), the National Institutes of Health (NIH) R15HL145573 (PI: Wei Li), the NIH R01HL129179 (PI: Anirban Sen Gupta, Co-I: Wei Li), the NIH R01HL130090 (PI: Thomas M McIntyre, Co-I: Wei Li), the West Virginia IDeA Network of Biomedical Research Excellence WV-INBRE (P20GM103434 to Gary Rankin), and the West Virginia Clinical and Translational Science Institute-Pop-Up COVID-19 Fund (to Wei Li) supported by the National Institute of General Medical Sciences (U54GM104942). Boyd Rorabaugh is supported by the NIH R15HL145546. The content is solely the responsibility of the authors and does not necessarily represent the official views of the NIH.

Disclosures

None.

Supplemental Material

Table S1

Figures S1–S5

Videos S1–S2

REFERENCES

1. Ismaiel A, Dumitraşcu DL. Cardiovascular risk in fatty liver disease: the liver-heart axis-literature review. *Front Med*. 2019;6:202. doi: [10.3389/fmed.2019.00202](https://doi.org/10.3389/fmed.2019.00202)
2. Roger VL, Weston SA, Redfield MM, Hellermann-Homan JP, Killian J, Yawn BP, Jacobsen SJ. Trends in heart failure incidence and survival in a community-based population. *JAMA*. 2004;292:344–350. doi: [10.1001/jama.292.3.344](https://doi.org/10.1001/jama.292.3.344)
3. Virani SS, Alonso A, Benjamin EJ, Bittencourt MS, Callaway CW, Carson AP, Chamberlain AM, Chang AR, Cheng S, Delling FN, et al. Heart disease and stroke statistics–2020 update: a report from the American Heart Association. *Circulation*. 2020;141:e1139–e596. doi: [10.1161/CIR.0000000000000757](https://doi.org/10.1161/CIR.0000000000000757)
4. Li W, Tanaka K, Ihaya A, Fujibayashi Y, Takamatsu S, Morioka K, Sasaki M, Uesaka T, Kimura T, Yamada N, et al. Gene therapy for chronic myocardial ischemia using platelet-derived endothelial cell growth factor in dogs. *Am J Physiol Heart Circ Physiol*. 2005;288:H408–H415. doi: [10.1152/ajpheart.00176.2004](https://doi.org/10.1152/ajpheart.00176.2004)
5. Lavu M, Gundewar S, Lefer DJ. Gene therapy for ischemic heart disease. *J Mol Cell Cardiol*. 2011;50:742–750. doi: [10.1016/j.yjmcc.2010.06.007](https://doi.org/10.1016/j.yjmcc.2010.06.007)
6. Rajagopalan S, Mohler ER 3rd, Lederman RJ, Mendelsohn FO, Saucedo JF, Goldman CK, Biebea J, Macko J, Kessler PD, Rasmussen HS, et al. Regional angiogenesis with vascular endothelial growth factor in peripheral arterial disease: a phase II randomized, double-blind, controlled study of adenoviral delivery of vascular endothelial growth factor 121 in patients with disabling intermittent claudication. *Circulation*. 2003;108:1933–1938. doi: [10.1161/01.CIR.0000093398.16124.29](https://doi.org/10.1161/01.CIR.0000093398.16124.29)
7. Chatterjee S, Stewart AS, Bish LT, Jayasankar V, Kim EM, Pirolli T, Burdick J, Woo YJ, Gardner TJ, Sweeney HL. Viral gene transfer of the antiapoptotic factor Bcl-2 protects against chronic posts ischemic heart failure. *Circulation*. 2002;106:1212–1217.
8. Otterbein LE, Foresti R, Motterlini R. Heme Oxygenase-1 and carbon monoxide in the heart: the balancing act between danger signaling and pro-survival. *Circ Res*. 2016;118:1940–1959. doi: [10.1161/CIRCRESAHA.116.306588](https://doi.org/10.1161/CIRCRESAHA.116.306588)
9. Daskalopoulos EP, Hermans KCM, van Delft L, Altara R, Blankesteijn WM. The role of inflammation in myocardial infarction. In: Blankesteijn WM, Altara R, eds. *Inflammation in Heart Failure*. Academic Press; 2015:39–65. doi: [10.1016/B978-0-12-800039-7.00003-7](https://doi.org/10.1016/B978-0-12-800039-7.00003-7)
10. Ridker PM, Everett BM, Thuren T, MacFadyen JG, Chang WH, Ballantyne C, Fonseca F, Nicolau J, Koenig W, Anker SD, et al. Antiinflammatory therapy with canakinumab for atherosclerotic disease. *N Engl J Med*. 2017;377:1119–1131. doi: [10.1056/NEJMoa1707914](https://doi.org/10.1056/NEJMoa1707914)
11. Ridker PM, Everett BM, Pradhan A, MacFadyen JG, Solomon DH, Zaharris E, Mam V, Hasan A, Rosenberg Y, Iturriga E, et al. Low-dose methotrexate for the prevention of atherosclerotic events. *N Engl J Med*. 2019;380:752–762. doi: [10.1056/NEJMoa1809798](https://doi.org/10.1056/NEJMoa1809798)
12. Tardif JC, Kouz S, Waters DD, Bertrand O, Diaz R, Maggioni AP, Pinto FJ, Ibrahim R, Gamra H, Kiwan GS, et al. Efficacy and safety of low-dose colchicine after myocardial infarction. *N Engl J Med*. 2019;381:2497–2505. doi: [10.1056/NEJMoa1912388](https://doi.org/10.1056/NEJMoa1912388)
13. Karantalis V, Hare JM. Use of mesenchymal stem cells for therapy of cardiac disease. *Circ Res*. 2015;116:1413–1430. doi: [10.1161/CIRCRESAHA.116.303614](https://doi.org/10.1161/CIRCRESAHA.116.303614)
14. Zimmert JM, Hare JM. Emerging role for bone marrow derived mesenchymal stem cells in myocardial regenerative therapy. *Basic Res Cardiol*. 2005;100:471–481. doi: [10.1007/s00395-005-0553-4](https://doi.org/10.1007/s00395-005-0553-4)
15. Liang X, Ding Y, Zhang Y, Tse H-F, Lian Q. Paracrine mechanisms of mesenchymal stem cell-based therapy: current status and perspectives. *Cell Transplant*. 2014;23:1045–1059. doi: [10.3727/096368913X667709](https://doi.org/10.3727/096368913X667709)
16. Figueroa FE, Carrion F, Villanueva S, Khoury M. Mesenchymal stem cell treatment for autoimmune diseases: a critical review. *Biol Res*. 2012;45:269–277. doi: [10.4067/S0716-97602012000300008](https://doi.org/10.4067/S0716-97602012000300008)
17. Martire A, Bedada FB, Uchida S, Poling J, Kruger M, Warnecke H, Richter M, Kubin T, Herold S, Braun T. Mesenchymal stem cells attenuate inflammatory processes in the heart and lung via inhibition of TNF signaling. *Basic Res Cardiol*. 2016;111:54. doi: [10.1007/s00395-016-0573-2](https://doi.org/10.1007/s00395-016-0573-2)
18. Kern S, Eichler H, Stoeve J, Kluter H, Bieback K. Comparative analysis of mesenchymal stem cells from bone marrow, umbilical cord blood, or adipose tissue. *Stem Cells*. 2006;24:1294–1301. doi: [10.1634/stemcells.2005-0342](https://doi.org/10.1634/stemcells.2005-0342)
19. von Bahr L, Batsis I, Moll G, Hägg M, Szakos A, Sundberg B, Uzunel M, Ringden O, Le Blanc K. Analysis of tissues following mesenchymal stromal cell therapy in humans indicates limited long-term engraftment and no ectopic tissue formation. *Stem Cells*. 2012;30:1575–1578. doi: [10.1002/stem.1118](https://doi.org/10.1002/stem.1118)
20. Li W, Yue H. Thymidine phosphorylase: a potential new target for treating cardiovascular disease. *Trends Cardiovasc Med*. 2018;28:157–171. doi: [10.1016/j.tcm.2017.10.003](https://doi.org/10.1016/j.tcm.2017.10.003)
21. Li W, Tanaka K, Morioka K, Takamori A, Handa M, Yamada N, Ihaya A. Long-term effect of gene therapy for chronic ischemic myocardium using platelet-derived endothelial cell growth factor in dogs. *J Gene Med*. 2008;10:412–420. doi: [10.1002/jgm.1156](https://doi.org/10.1002/jgm.1156)
22. Li W, Tanaka K, Morioka K, Uesaka T, Yamada N, Takamori A, Handa M, Tanabe S, Ihaya A. Thymidine phosphorylase gene transfer inhibits vascular smooth muscle cell proliferation by upregulating heme oxygenase-1 and p27KIP1. *Arterioscler Thromb Vasc Biol*. 2005;25:1370–1375. doi: [10.1161/01.ATV.0000168914.85107.64](https://doi.org/10.1161/01.ATV.0000168914.85107.64)
23. Handa M, Li W, Morioka K, Takamori A, Yamada N, Ihaya A. Adventitial delivery of platelet-derived endothelial cell growth factor gene prevented intimal hyperplasia of vein graft. *J Vasc Surg*. 2008;48:1566–1574. doi: [10.1016/j.jvs.2008.07.029](https://doi.org/10.1016/j.jvs.2008.07.029)
24. Yue H, Tanaka K, Furukawa T, Karnik SS, Li W. Thymidine phosphorylase inhibits vascular smooth muscle cell proliferation via upregulation of STAT3. *Biochim Biophys Acta*. 2012;1823:1316–1323. doi: [10.1016/j.bbamer.2012.05.025](https://doi.org/10.1016/j.bbamer.2012.05.025)
25. Cheng Y, Rong J. Therapeutic potential of heme oxygenase-1/carbon monoxide system against ischemia-reperfusion injury. *Curr Pharm Des*. 2017;23:3884–3898. doi: [10.2174/1381612823666170413122439](https://doi.org/10.2174/1381612823666170413122439)
26. Li W, Gigante A, Perez-Perez MJ, Yue H, Hirano M, McIntyre TM, Silverstein RL. Thymidine phosphorylase participates in platelet signaling and promotes thrombosis. *Circ Res*. 2014;115:997–1006. doi: [10.1161/CIRCRESAHA.115.304591](https://doi.org/10.1161/CIRCRESAHA.115.304591)
27. Belcher A, Zulfiker AHM, Li OQ, Yue H, Gupta AS, Li W. Targeting thymidine phosphorylase with tipiracil hydrochloride attenuates thrombosis without increasing risk of bleeding in mice. *Arterioscler Thromb Vasc Biol*. 2021;41:668–682. doi: [10.1161/atvbaha.120.315109](https://doi.org/10.1161/atvbaha.120.315109)
28. Lopez LC, Akman HO, Garcia-Cazorla A, Dorado B, Marti R, Nishino I, Tadesse S, Pizzorno G, Shungu D, Bonilla E, et al. Unbalanced deoxy nucleotide pools cause mitochondrial DNA instability in thymidine phosphorylase-deficient mice. *Hum Mol Genet*. 2009;18:714–722. doi: [10.1093/hmg/ddn401](https://doi.org/10.1093/hmg/ddn401)
29. Li W, Kennedy D, Shao Z, Wang X, Kamdar AK, Weber M, Mislick K, Kiefer K, Morales R, Agatista-Boyle B, et al. Paraoxonase 2 prevents the development of heart failure. *Free Radic Biol Med*. 2018;121:117–126. doi: [10.1016/j.freeradbiomed.2018.04.583](https://doi.org/10.1016/j.freeradbiomed.2018.04.583)
30. Pachon RE, Scharf BA, Vatner DE, Vatner SF. Best anesthetics for assessing left ventricular systolic function by echocardiography in mice. *Am J Physiol Heart Circ Physiol*. 2015;308:H1525–H1529. doi: [10.1152/ajpheart.00890.2014](https://doi.org/10.1152/ajpheart.00890.2014)
31. Ohtani T, Mohammed SF, Yamamoto K, Dunlay SM, Weston SA, Sakata Y, Rodeheffer RJ, Roger VL, Redfield MM. Diastolic stiffness as assessed by diastolic wall strain is associated with adverse remodeling and poor outcomes in heart failure with preserved ejection fraction. *Eur Heart J*. 2012;33:1742–1749. doi: [10.1093/eurheartj/ehs135](https://doi.org/10.1093/eurheartj/ehs135)
32. Selvaraj S, Aguilar FG, Martinez EE, Beussink L, Kim KY, Peng J, Lee DC, Patel A, Sha J, Irvin MR, et al. Diastolic wall strain: a simple marker of abnormal cardiac mechanics. *Cardiovasc Ultrasound*. 2014;12:40. doi: [10.1186/1476-7120-12-40](https://doi.org/10.1186/1476-7120-12-40)
33. Waterson RE, Thompson CG, Mabe NW, Kaur K, Talbot JN, Neubig RR, Rorabaugh BR. Gα(i2)-mediated protection from ischaemic injury is modulated by endogenous RGS proteins in the mouse heart. *Cardiovasc Res*. 2011;91:45–52. doi: [10.1093/cvr/cvr054](https://doi.org/10.1093/cvr/cvr054)
34. Du L, Yu Y, Ma H, Lu X, Ma L, Jin Y, Zhang H. Hypoxia enhances protective effect of placental-derived mesenchymal stem cells on damaged

- intestinal epithelial cells by promoting secretion of insulin-like growth factor-1. *Int J Mol Sci*. 2014;15:1983–2002. doi: 10.3390/ijms15021983
35. Bunnell BA, Flaat M, Gagliardi C, Patel B, Ripoll C. Adipose-derived stem cells: isolation, expansion and differentiation. *Methods*. 2008;45:115–120. doi: 10.1016/j.jymeth.2008.03.006
 36. Mosmann T. Rapid colorimetric assay for cellular growth and survival: application to proliferation and cytotoxicity assays. *J Immunol Methods*. 1983;65:55–63. doi: 10.1016/0022-1759(83)90303-4
 37. Liu L, Yu Q, Fu S, Wang B, Hu K, Wang L, Hu Y, Xu Y, Yu X, Huang H. CXCR4 antagonist AMD3100 promotes mesenchymal stem cell mobilization in rats preconditioned with the hypoxia-mimicking agent cobalt chloride. *Stem Cells Dev*. 2018;27:466–478. doi: 10.1089/scd.2017.0191
 38. Li W, Chiba Y, Kimura T, Morioka K, Uesaka T, Ihaya A, Muraoka R. Transmyocardial laser revascularization induced angiogenesis correlated with the expression of matrix metalloproteinases and platelet-derived endothelial cell growth factor. *Eur J Cardiothorac Surg*. 2001;19:156–163. doi: 10.1016/S1010-7940(00)00649-7
 39. Li W, Tanaka K, Chiba Y, Kimura T, Morioka K, Uesaka T, Ihaya A, Sasaki M, Tsuda T, Yamada N. Role of MMPs and plasminogen activators in angiogenesis after transmyocardial laser revascularization in dogs. *Am J Physiol Heart Circ Physiol*. 2003;284:H23–H30. doi: 10.1152/ajpheart.00240.2002
 40. Yue H, Lee JD, Shimizu H, Uzui H, Mitsuke Y, Ueda T. Effects of magnesium on the production of extracellular matrix metalloproteinases in cultured rat vascular smooth muscle cells. *Atherosclerosis*. 2003;166:271–277. doi: 10.1016/s0021-9150(02)00390-8
 41. Yue H, Uzui H, Lee JD, Shimizu H, Ueda T. Effects of magnesium on matrix metalloproteinase-2 production in cultured rat cardiac fibroblasts. *Basic Res Cardiol*. 2004;99:257–263. doi: 10.1007/s00395-004-0472-9
 42. Bagher P, Segal SS. The mouse cremaster muscle preparation for intravital imaging of the microcirculation. *J Vis Exp*. 2011;2874. doi: 10.3791/2874
 43. Li W, McIntyre TM, Silverstein RL. Ferric chloride-induced murine carotid arterial injury: a model of redox pathology. *Redox Biol*. 2013;1:50–55. doi: 10.1016/j.redox.2012.11.001
 44. Li W, Nieman M, Sen GA. Ferric chloride-induced murine thrombosis models. *J Vis Exp*. 2016;54479. doi: 10.3791/54479
 45. Gao E, Lei YH, Shang X, Huang ZM, Zuo L, Boucher M, Fan Q, Chuprun JK, Ma XL, Koch WJ. A novel and efficient model of coronary artery ligation and myocardial infarction in the mouse. *Circ Res*. 2010;107:1445–1453. doi: 10.1161/CIRCRESAHA.110.223925
 46. Lindsey ML, Kassiri Z, Virag JAI, de Castro Brás LE, Scherrer-Crosbie M. Guidelines for measuring cardiac physiology in mice. *Am J Physiol Heart Circ Physiol*. 2018;314:H733–h752. doi: 10.1152/ajpheart.00339.2017
 47. Zhang H, Chen X, Gao E, MacDonnell SM, Wang W, Kolpakov M, Nakayama H, Zhang X, Jaleel N, Harris DM, et al. Increasing cardiac contractility after myocardial infarction exacerbates cardiac injury and pump dysfunction. *Circ Res*. 2010;107:800–809. doi: 10.1161/CIRCRESAHA.110.219220
 48. Dorn GW, Molkenin JD. Manipulating cardiac contractility in heart failure. *Circulation*. 2004;109:150–158. doi: 10.1161/01.CIR.0000111581.15521.F5
 49. Liehn EA, Postea O, Curaj A, Marx N. Repair after myocardial infarction, between fantasy and reality: the role of chemokines. *J Am Coll Cardiol*. 2011;58:2357–2362. doi: 10.1016/j.jacc.2011.08.034
 50. Ziegler M, Wang X, Peter K. Platelets in cardiac ischaemia/reperfusion injury: a promising therapeutic target. *Cardiovasc Res*. 2019;115:1178–1188. doi: 10.1093/cvr/cvz070
 51. Waguri Y, Otsuka T, Sugimura I, Matsui N, Asai K, Moriyama A, Kato T. Gliostatin/platelet-derived endothelial cell growth factor as a clinical marker of rheumatoid arthritis and its regulation in fibroblast-like synoviocytes. *Br J Rheumatol*. 1997;36:315–321. doi: 10.1093/rheumatology/36.3.315
 52. Toyoda Y, Tabata S, Kishi J, Kuramoto T, Mitsuhashi A, Saijo A, Kawano H, Goto H, Aono Y, Hanibuchi M, et al. Thymidine phosphorylase regulates the expression of CXCL10 in rheumatoid arthritis fibroblast-like synoviocytes. *Arthritis Rheumatol*. 2014;66:560–568. doi: 10.1002/art.38263
 53. Rahmati M, Petitbarat M, Dubanchet S, Bensussan A, Chaouat G, Ledee N. Granulocyte-colony stimulating factor related pathways tested on an endometrial ex-vivo model. *PLoS One*. 2014;9:e102286. doi: 10.1371/journal.pone.0102286
 54. Prabhu SD, Frangogiannis NG. The biological basis for cardiac repair after myocardial infarction. *Circ Res*. 2016;119:91–112. doi: 10.1161/CIRCRESAHA.116.303577
 55. Elsasser A, Schlepfer M, Klovekorn WP, Cai WJ, Zimmermann R, Müller KD, Strasser R, Kostin S, Gagel C, Munkel B, et al. Hibernating myocardium: an incomplete adaptation to ischemia. *Circulation*. 1997;96:2920–2931. doi: 10.1161/01.cir.96.9.2920
 56. Hamou C, Callaghan MJ, Thangarajah H, Chang E, Chang EI, Grogan RH, Paterno J, Vial IN, Jazayeri L, Gurtner GC. Mesenchymal stem cells can participate in ischemic neovascularization. *Plast Reconstr Surg*. 2009;123:45S–55S. doi: 10.1097/PRS.0b013e318191be4a
 57. Pula G, Mayr U, Evans C, Prokopi M, Vara DS, Yin X, Astrouklakis Z, Xiao Q, Hill J, Xu Q, et al. Proteomics identifies thymidine phosphorylase as a key regulator of the angiogenic potential of colony-forming units and endothelial progenitor cell cultures. *Circ Res*. 2009;104:32–40. doi: 10.1161/CIRCRESAHA.108.182261
 58. Broxmeyer HE. Chemokines in hematopoiesis. *Curr Opin Hematol*. 2008;15:49–58. doi: 10.1097/MOH.0b013e3182f29012
 59. Hill JM, Zalos G, Halcox JP, Schenke WH, Waclawiw MA, Quyyumi AA, Finkel T. Circulating endothelial progenitor cells, vascular function, and cardiovascular risk. *N Engl J Med*. 2003;348:593–600. doi: 10.1056/NEJMoa022287
 60. Fu X, Liu G, Halim A, Ju Y, Luo Q, Song AG. Mesenchymal stem cell migration and tissue repair. *Cell*. 2019;8:8. doi: 10.3390/cells8080784
 61. Nitzsche F, Müller C, Lukomska B, Jolkonen J, Deten A, Boltze J. Concise review: MSC adhesion cascade—insights into homing and transendothelial migration. *Stem Cells*. 2017;35:1446–1460. doi: 10.1002/stem.2614
 62. Bento D, Lopes S, Maia I, Lima R, Miranda JM. Bubbles moving in blood flow in a microchannel network: the effect on the local hematocrit. *Micromachines (Basel)*. 2020;11:344. doi: 10.3390/mi1040344
 63. Bonvini RF, Hendiri T, Camenzind E. Inflammatory response post-myocardial infarction and reperfusion: a new therapeutic target? *Eur Heart J Suppl*. 2005;7:127–136. doi: 10.1093/eurheartj/sui077
 64. Cheng K, Shen D, Xie Y, Cingolani E, Malliaras K, Marbán E. Brief report: mechanism of extravasation of infused stem cells. *Stem cells*. 2012;30:2835–2842. doi: 10.1002/stem.1184
 65. Huang G, Lu H, Hao A, Ng DCH, Ponniah S, Guo K, Lufe C, Zeng Q, Cao X. GRIM-19, a cell death regulatory protein, is essential for assembly and function of mitochondrial complex I. *Mol Cell Biol*. 2004;24:8447–8456. doi: 10.1128/MCB.24.19.8447-8456.2004
 66. Kalogeris T, Baines CP, Krenz M, Korhuis RJ. Cell biology of ischemia/reperfusion injury. *Int Rev Cell Mol Biol*. 2012;298:229–317. doi: 10.1016/b978-0-12-394309-5.00006-7
 67. Severino P, D'Amato A, Pucci M, Infusino F, Adamo F, Birtolo LI, Netti L, Montefusco G, Chimenti C, Lavalle C, et al. Ischemic heart disease pathophysiology paradigms overview: from plaque activation to microvascular dysfunction. *Int J Mol Sci*. 2020;21:21. doi: 10.3390/ijms21218118
 68. Johnson T, Zhao L, Manuel G, Taylor H, Liu D. Approaches to therapeutic angiogenesis for ischemic heart disease. *J Mol Med (Berl)*. 2019;97:141–151. doi: 10.1007/s00109-018-1729-3
 69. Ylä-Herttuala S, Bridges C, Katz MG, Korpisalo P. Angiogenic gene therapy in cardiovascular diseases: dream or vision? *Eur Heart J*. 2017;38:1365–1371. doi: 10.1093/eurheartj/ehw547
 70. Yamada N, Li W, Ihaya A, Kimura T, Morioka K, Uesaka T, Takamori A, Handa M, Tanabe S, Tanaka K. Platelet-derived endothelial cell growth factor gene therapy for limb ischemia. *J Vasc Surg*. 2006;44:1322–1328. doi: 10.1016/j.jvs.2006.07.051
 71. Brown NS, Bicknell R. Thymidine phosphorylase, 2-deoxy-D-ribose and angiogenesis. *Biochem J*. 1998;334:1–8. doi: 10.1042/bj3340001
 72. Elamin YY, Rafee S, Osman N, O Byrne KJ, Gately K. Thymidine phosphorylase in cancer; enemy or friend? *Cancer Microenviron*. 2016;9:33–43. doi: 10.1007/s12307-015-0173-y
 73. Camici PG, d'Amati G, Rimoldi O. Coronary microvascular dysfunction: mechanisms and functional assessment. *Nat Rev Cardiol*. 2015;12:48–62. doi: 10.1038/nrcardio.2014.160
 74. Ong SB, Hernandez-Resendiz S, Crespo-Avilan GE, Mukhametshina RT, Kwek XY, Cabrera-Fuentes HA, Hausenloy DJ. Inflammation following acute myocardial infarction: multiple players, dynamic roles, and novel therapeutic opportunities. *Pharmacol Ther*. 2018;186:73–87. doi: 10.1016/j.pharmthera.2018.01.001
 75. van der Meijden PEJ, Heemskerk JWM. Platelet biology and functions: new concepts and clinical perspectives. *Nat Rev Cardiol*. 2019;16:166–179. doi: 10.1038/s41569-018-0110-0

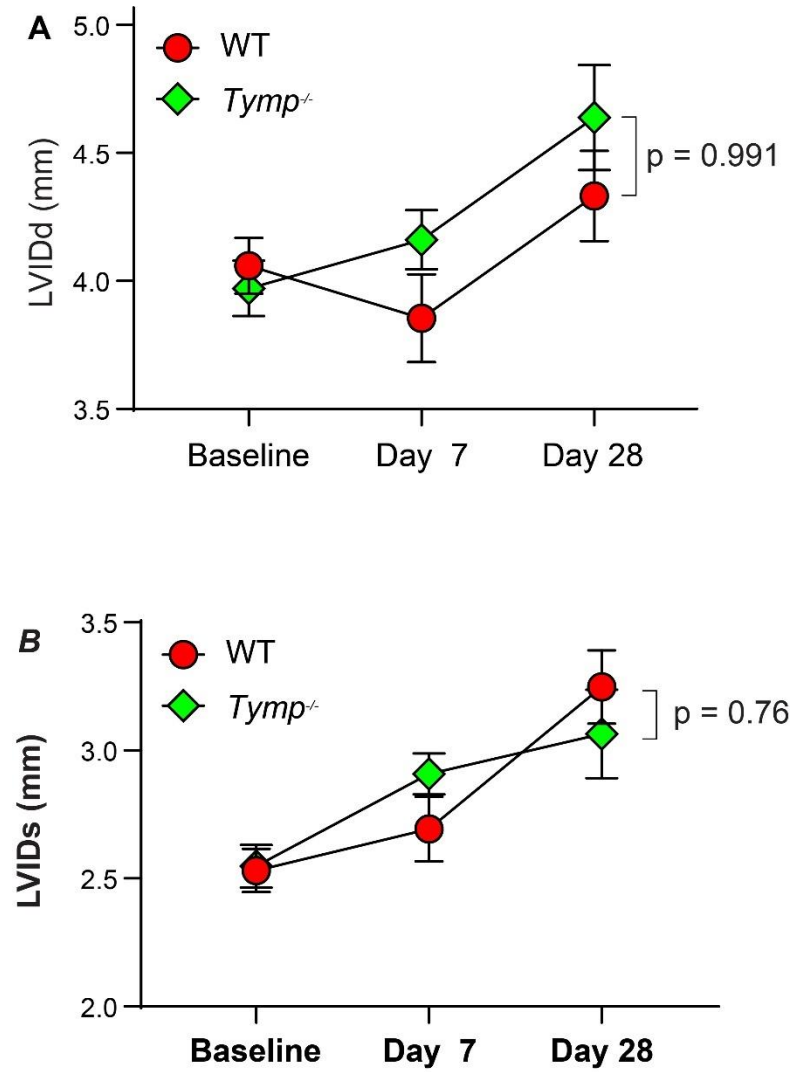
76. Subramaniam S, Scharrer I. Procoagulant activity during viral infections. *Front Biosci (Landmark Ed)*. 2018;23:1060–1081. doi: [10.2741/4633](https://doi.org/10.2741/4633)
77. Haque N, Rahman MT, Abu Kasim NH, Alabsi AM. Hypoxic culture conditions as a solution for mesenchymal stem cell based regenerative therapy. *ScientificWorldJournal*. 2013;2013:632972. doi: [10.1155/2013/632972](https://doi.org/10.1155/2013/632972)
78. Li J, Hu S, Zhu D, Huang K, Mei X, Abad BLJ, Cheng K. All roads lead to Rome (the heart): cell retention and outcomes from various delivery routes of cell therapy products to the heart. *J Am Heart Assoc*. 2021;10:e020402. doi: [10.1161/JAHA.120.020402](https://doi.org/10.1161/JAHA.120.020402)
79. Campbell NG, Kaneko M, Shintani Y, Narita T, Sawhney V, Coppen SR, Yashiro K, Mathur A, Suzuki K. Cell size critically determines initial retention of bone marrow mononuclear cells in the heart after intracoronary injection: evidence from a rat model. *PLoS One*. 2016;11:e0158232. doi: [10.1371/journal.pone.0158232](https://doi.org/10.1371/journal.pone.0158232)
80. Vincent LG, Choi YS, Alonso-Latorre B, del Álamo JC, Engler AJ. Mesenchymal stem cell durotaxis depends on substrate stiffness gradient strength. *Biotechnol J*. 2013;8:472–484. doi: [10.1002/biot.201200205](https://doi.org/10.1002/biot.201200205)
81. Lachowski D, Cortes E, Rice A, Pinato D, Rombouts K, Del Rio HA. Matrix stiffness modulates the activity of MMP-9 and TIMP-1 in hepatic stellate cells to perpetuate fibrosis. *Sci Rep*. 2019;9:7299. doi: [10.1038/s41598-019-43759-6](https://doi.org/10.1038/s41598-019-43759-6)
82. Koh SH, Lo EH. The role of the PI3K pathway in the regeneration of the damaged brain by neural stem cells after cerebral infarction. *J Clin Neurol*. 2015;11:297–304. doi: [10.3988/jcn.2015.11.4.297](https://doi.org/10.3988/jcn.2015.11.4.297)
83. Samakova A, Gazova A, Sabova N, Valaskova S, Jurikova M, Kyselovic J. The PI3k/Akt pathway is associated with angiogenesis, oxidative stress and survival of mesenchymal stem cells in pathophysiologic condition in ischemia. *Physiol Res*. 2019;68:S131–s138. doi: [10.33549/physiolres.934345](https://doi.org/10.33549/physiolres.934345)
84. Seung H, Wrobel J, Wadle C, Bühler T, Chiang D, Rettkowski J, Cabezas-Wallscheid N, Hechler B, Stachon P, Maier A, et al. P2Y12-dependent activation of hematopoietic stem and progenitor cells promotes emergency hematopoiesis after myocardial infarction. *Basic Res Cardiol*. 2022;117:16. doi: [10.1007/s00395-022-00927-6](https://doi.org/10.1007/s00395-022-00927-6)
85. Hwang SN, Kim JC, Kim SY. Heterogeneity of GRIM-19 expression in the adult mouse brain. *Cell Mol Neurobiol*. 2019;39:935–951. doi: [10.1007/s10571-019-00689-1](https://doi.org/10.1007/s10571-019-00689-1)
86. Zacchigna S, Paldino A, Falcao-Pires I, Daskalopoulos EP, Dal Ferro M, Vodret S, Lesizza P, Cannata A, Miranda-Silva D, Lourenco AP, et al. Towards standardization of echocardiography for the evaluation of left ventricular function in adult rodents: a position paper of the ESC Working Group on Myocardial Function. *Cardiovasc Res*. 2021;117:43–59. doi: [10.1093/cvr/cvaa110](https://doi.org/10.1093/cvr/cvaa110)

SUPPLEMENTAL MATERIAL

Table S1. Real-time PCR primers for testing mouse genes related to inflammation.

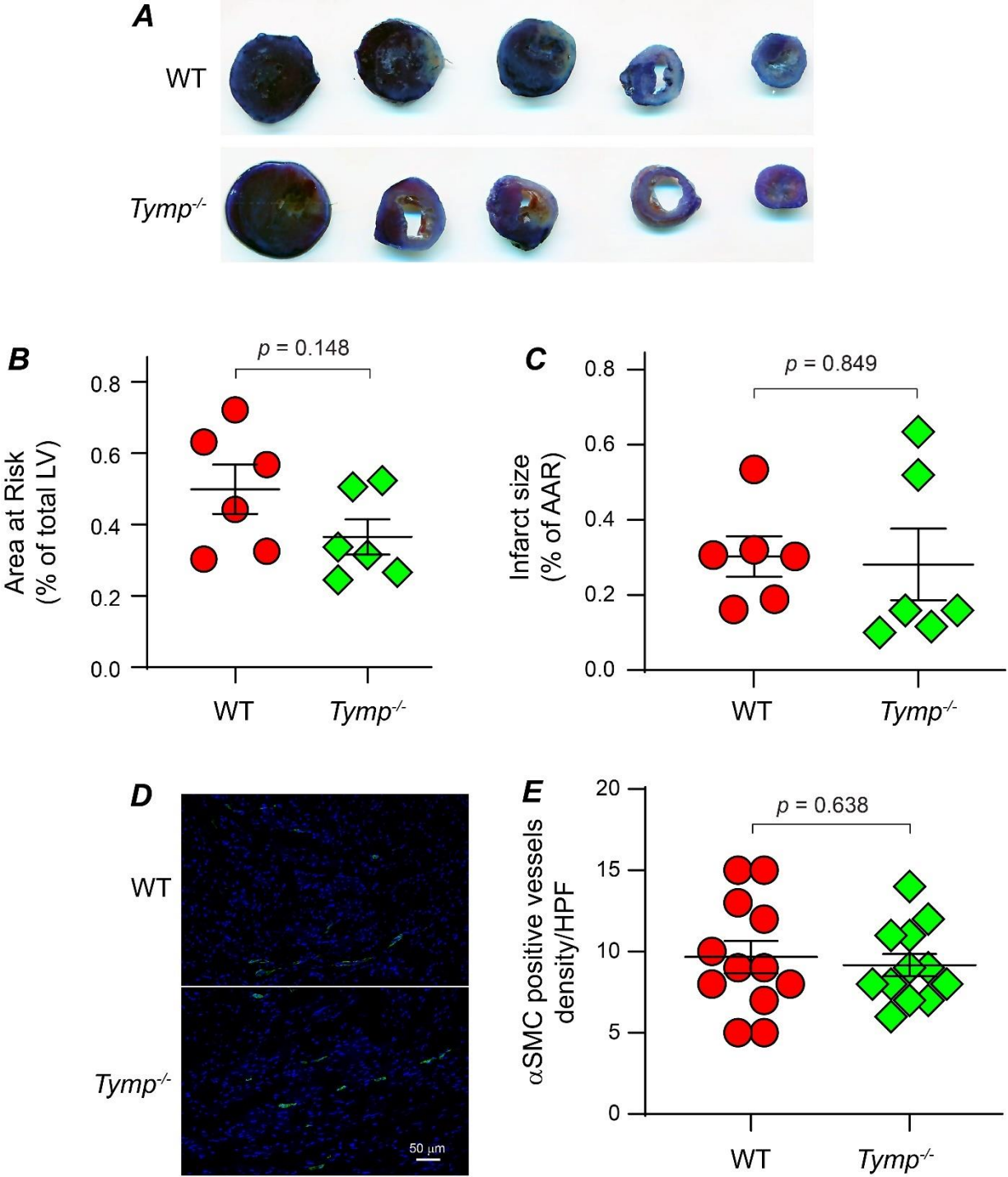
Targets	Forward Sequence (5'-3')	Reverse Sequence (5'-3')
CD11b	TCAGCAGGAGAGTGACATTGT	TGTGATCTTGGGCTAGGGTTT
Cd68	CCCCACCTGTCTCTCTCATTT	CATTGTATTCCACCGCCATGT
IL-1 β	GACGGACCCCAAAGATGAAG	CAATGAGTGATACTGCCTGCC
IL-4	AAGCTGCACCATGAATGAGTC	ATGGTGGCTCAGTACTACGAG
IL-6	TGCAAGAGACTTCCATCCAGT	CAGGTCTGTTGGGAGTGGTAT
Cxcl10	AAGTGCTGCCGTCATTTTCTG	ATTCAAGCTTCCCTATGGCC
Icam-1	TCGATCTTCCAGCTACCATCC	CTCCCAGCTCCAGGTATATCC
MCP-1(CCL2)	AGGTCCCTGTCATGCTTCTG	TGGGATCATCTTGCTGGTGA
TLR-2	CCTGTGTTGCTGGTCATGAAA	AAGGATAGGAGTTCGCAGGAG
TLR-4	CTGCCAACATCATCCAGGAAG	CTGCTCAGAACTGCCATGTT
Tnf- α	GCCTCTTCTCATTCCCTGCTTG	TGATCTGAGTGTGAGGGTCTG
GAPDH	CAGCAACTCCCACTCTTCCACCTTCG	GGCCTCTCTTGCTCAGTGTCTTGCT

Figure S1. TYMP deficiency has no effect on cardiac remodeling.



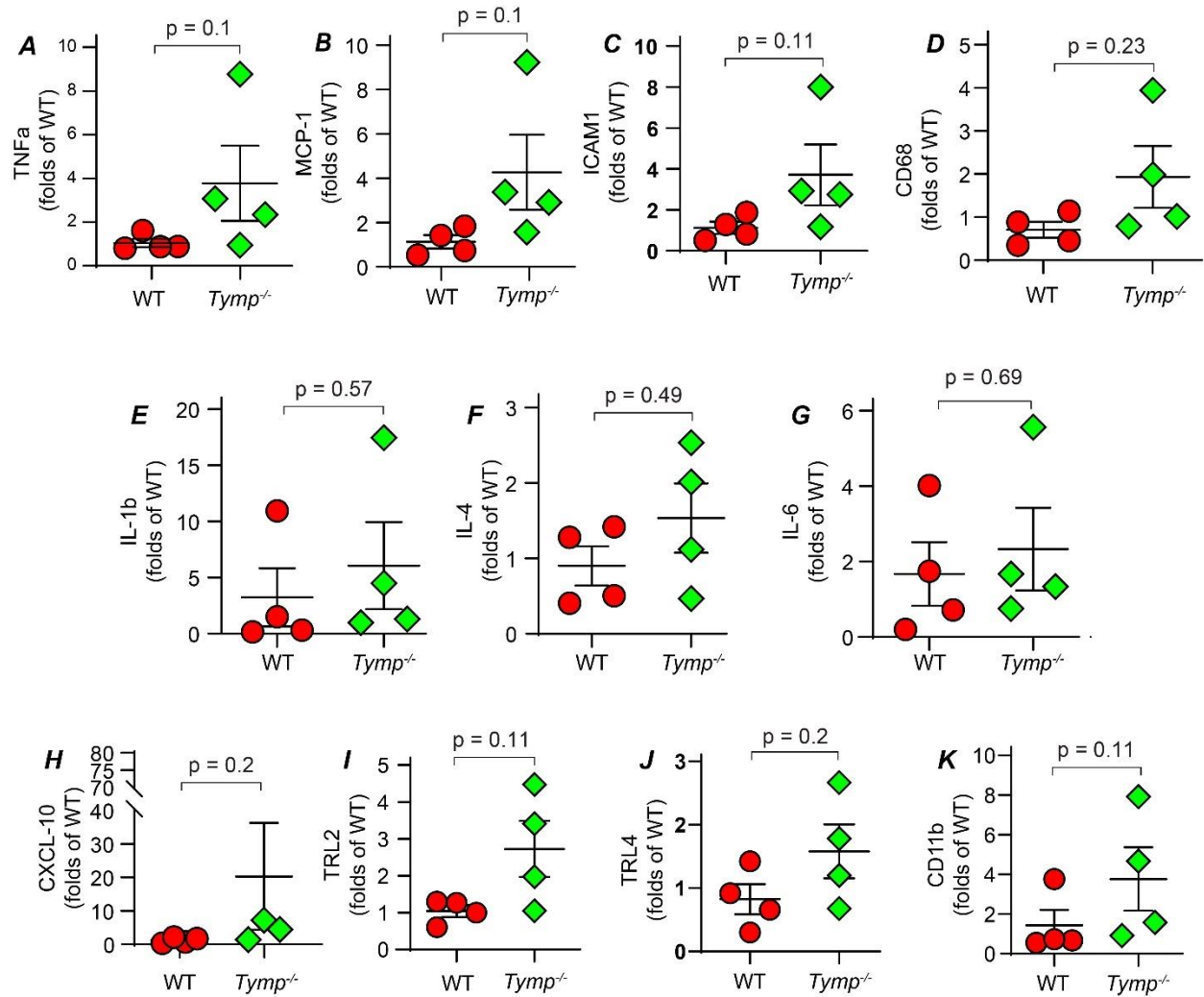
Age matched male wild type C57BL/6J (WT) and *Tymp*^{-/-} mice were subjected to the LAD ligation, a mouse myocardial infarction model. **A.** LVIDd and **B.** LVIDs data are shown as mean \pm SE. Mixed-effects two-factor ANOVA. n = 7-12.

Figure S2. TYMP deficiency in mice does not affect areas at risk (AAR) at the early phase following left anterior descending coronary artery (LAD) ligation.



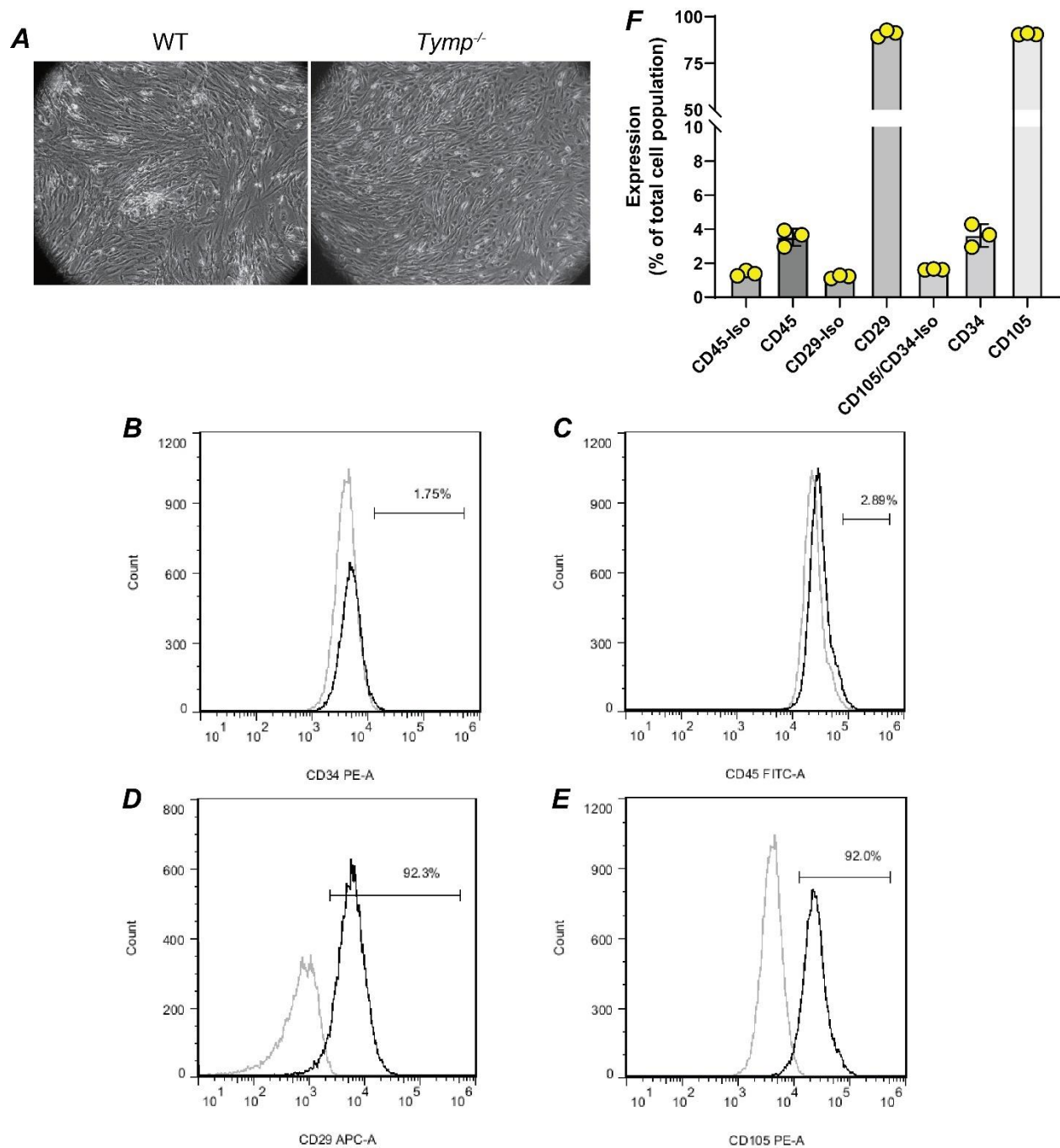
Age matched male wild type C57BL/6J (WT) and *Tymp*^{-/-} mice were subjected to LAD ligation. **A.** AAR and infarct size were assessed 18 hours post LAD ligation by Evans blue perfusion and triphenyl tetrazolium chloride (TTC) staining. **B.** AAR was defined as [ischemic zone (pink) + infarct zone (pale)]/total left ventricle area x 100%. **C.** Infarct size was presented as ratio of area of infarction (pale) to AAR. Student's t-test was used for statistical analyses. **D & E.** Mice were sacrificed 24 h after LAD ligation. The hearts were removed and frozen hearts were cross-sectioned from apex to the level of LAD ligation. Two sections at similar levels were randomly selected from each mouse and stained for α -smooth muscle actin (α -SMA, green). Nuclei were stained with DAPI. Two images (20 x) were randomly taken from each section and α -SMA positive small arteries were counted. The bar graph represents accumulated data from 3 mice, 2 sections from each mouse. Student's t-test. Scale bar = 50 μ m.

Figure S3. TYMP deficiency does not affect inflammation in hearts 3 days post-infarction.



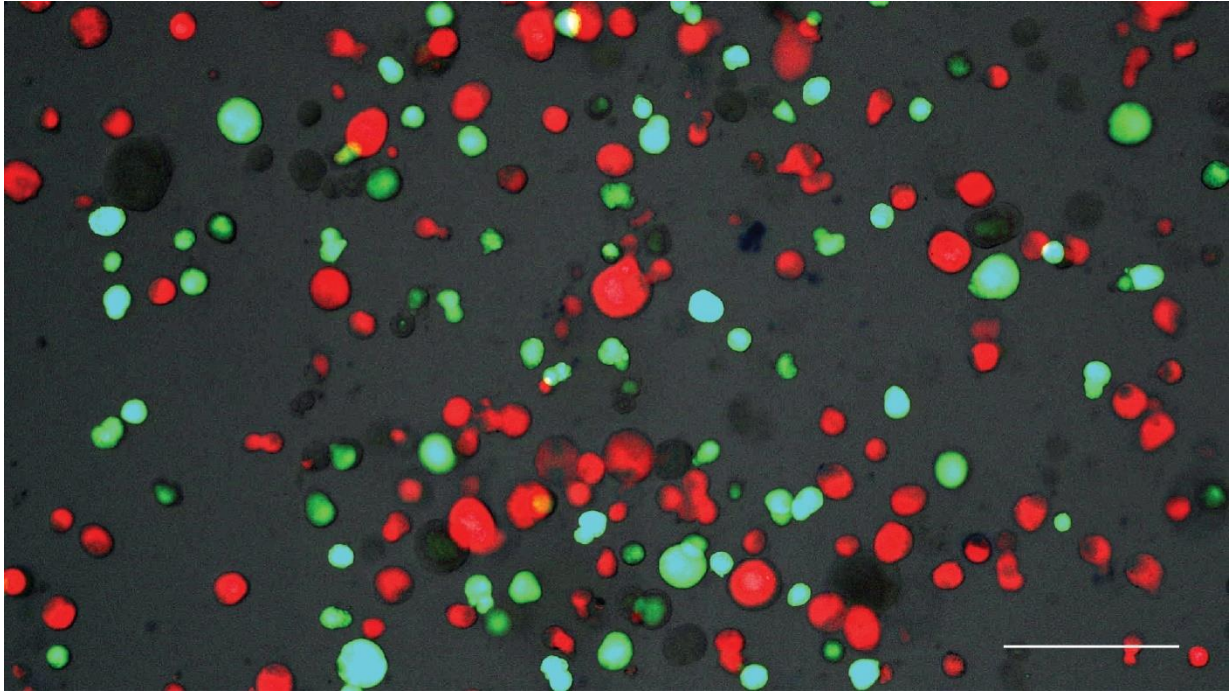
Myocardial tissue in the infarction zone on day 3 post-AMI were used for total RNA extraction. qPCR was used to quantitatively analyze the expression of the indicated molecules. Data were adjusted to the housekeeping gene, GAPDH, and presented as fold change of the average value of WT samples used. Mann Whitney test was used to compare the change between groups; n = 4.

Figure S4. Characterization of Mesenchymal Stem Cells.



A. Image of WT and *Tymp*^{-/-} MSCs when they reached to a confluence. **B - D.** Flow cytometry analyses of MSC surface markers. Gray lines indicate staining with isotype control IgG. Black lines indicate staining with the specific antibody as indicated in each panel. **F.** Accumulating data of panels B to D, n = 3.

Figure S5. WT and *Tymp*^{-/-} MSCs were labeled with Cell Tracker green and red, respectively.



An equal number of the cells were mixed together for injection. One drop of the mixture was dropped on a slide glass, covered with one piece of cover slip and images were taken using a fluorescence microscope. Scale bar = 50 μm .

Supplemental Video Legends:

Video S1. Leukocytes and platelets were isolated from donor mice and labeled with CellTracker™ Green CMFDA and CellTracker™ Red CMTPX, respectively. The fluorescently labeled leukocytes and platelets were washed with PBS to remove free dyes, mixed together, resuspended in 150 μ L saline, and injected into male recipient mice through the jugular vein. TNF α (500 ng in 100 μ L saline) was given to the recipient mice by intrascrotal injection, immediately after they received the injection of the leukocyte and platelet mixture. Three hours later, cremaster muscle microcirculation model was prepared. Microvessels were screened and the formation of microthrombi was examined by intravital microscopy. Best viewed with Windows Media Player.

Video S2 (WT) and Video S3 (*Tymp*^{-/-}). Cellix flow chambers were coated with type I collagen, fibronectin, and bovine serum albumin at a final concentration at 30, 10, and 10 μ g/mL in PBS, respectively. MSCs re-suspended in full complete media at a concentration of 10^5 cells/mL were stained with Rhodamine 6G at a final concentration of 50 μ g/mL, and then perfused through the flow chamber at a flow rate of 10 μ L/min for three minutes. The chamber was washed with PBS in the same flow rate for three minutes to remove all non-attached cells and all adhered cells were counted over the chamber. Best viewed with Windows Media Player.